TABLE I. Profiles of Patients Who Underwent Hematopoietic Stem Cell Transplantation

	EBV-HLH	FHL	*P*-value
Number, male:female	14, 4:10	43, 23:20	0.37
Age at onset (median, range)	5.5y, 6m–18y	0.5y, 6d–12y	<0.0001
Age at SCT (median, range)	5.9y, 1.4–18y	1.2y, 0.4–15y	0.0002
Observation period (median, range)	5.5y, 0.3–16y	4.8y, 0.2–19y	0.94
Manifestation at diagnosis (%)			
Fever	100	95	>0.99
Hepatosplenomegaly	86	86	>0.99
Lymphadenopathy	36	21	0.30
Skin eruption	7	14	0.67
Respiratory failure	36	14	0.12
DIC	50	33	0.26
Treatment prior to SCT (%)			
HLH94 only	36 (5/14)	60 (25/42)	0.14
Multidrug chemotherapy	57 (8/14)	19 (8/42)	0.017
Diagnosis to SCT (median, range)	5.8m, 1.8–24m	7.5m, 1.6–84m	0.18
SCT (n)			
Allogeneic	11	42	
Auto/Identical twin	3	1	
Nucleated cell doses ($\times 10^8$/kg)	1.3 (0.2–6.6)	2.5 (0.1–12.7)	0.14
Donor			
UCB	7	21	0.94
Others	7	22	
HLA disparity no	4	28	0.09
HLA disparity yes (>1 locus[a])	7	14	
Conditioning			
Myeloablative[b]	11	31	>0.99
RIC[c]	3	11	
Irradiation yes	4	11	0.73
Irradiation no	9	31	
ATG yes	0	8	0.18
ATG no	14	34	
CNS abnormality (%)			
At diagnosis	29[d] (4/14)	21[d] (9/42)	0.72
Before SCT	57 (8/14)	67 (28/42)	0.52
CSF pleocytosis	25 (2/8)	32 (7/22)	>0.99
MRI abnormality	36 (5/14)	51 (20/39)	0.36
Convulsion	43 (6/14)	41 (17/41)	0.93
Disturbed consciousness	36 (5/14)	24 (10/41)	0.49
Post-transplant state (n)			
Early death (<100 days)	2	7	0.48
Alive	12	29	0.31
Neurological deficit (%)	8[d] (1/12)	29[d] (7/24)	0.22
Late sequelae[e] (%)	8 (1/12)	52 (11/21)	0.022

ATG, anti-thymocyte globulin; BU, busulfan; CNS, central nervous system; CSF, cerebrospinal fluid; CY, cyclophosphamide; DIC, disseminated intravascular coagulopathy; EBV, Epstein–Barr virus; FHL, familial hemophagocytic lymphohistiocytosis; FLU, fludarabine; HLH, hemophagocytic lymphohistiocytosis; MEL, melphalan; MRI, magnetic resonance imaging; SCT, hematopoietic stem cell transplantation; TAI, thoracoabdominal irradiation; TBI, total body irradiation; UCBT, unrelated donor cord blood transplantation; VP16, etoposide. Parenthesis means the positive number of patients per the evaluable number of patients. The observation period means the time from the onset to the last visit or death. [a]Human leukocyte antigen (HLA) disparity was assessed by the serotyping data of HLA-A, -B, and -DR; [b]Myeloablative conditionings for EBV-HLH were VP16/BU/CY 8 (4 in UCBT) and others 3, and those for FHL were VP16/BU/CY + ATG 23 (10 in UCBT) and others 8; [c]Reduced intensity conditionings (RIC) for EBV-HLH were MEL/FLU + TAI 3 (2 in UCBT), and those for FHL were MEL/FLU + low dose TBI + ATG 8 (4 in UCBT) and others 3; [d]The proportion of patients having neurological abnormality was lower in survived patients with EBV-HLH ($P = 0.0015$). Survived patients were neurodevelopmentally assessed at the last visit to the hospital; [e]Late sequela(e) in EBV-HLH was hemiparesis (n = 1), and those in FHL were short stature (n = 5), endocrinological abnormality (n = 1), psychomotor retardation with or without seizure (n = 5), brain atrophy (n = 1), and hearing difficulty (n = 1).

2008. An analysis of the risk factors for SCT outcome was possible for FHL, but not for EBV-HLH because of the small number of subjects. Age at onset of HLH or at the SCT, duration from the onset to SCT, CNS disease before SCT, donor sources, and the type of conditioning were tested using the log-rank method. Cox proportional-hazard model was employed to examine the association between selected clinical variables and the risk for death. A logistic regression model was used to investigate factors associated with neurological sequelae. Chi-square test or Fisher's exact test were employed in other comparisons. P values less than 0.05 were considered to be significant.

RESULTS

Profiles of EBV-HLH and FHL Patients

A comparison of the clinical profiles (Table I) revealed that the ages at disease onset and at the time of SCT were each higher in EBV-HLH than in FHL patients ($P < 0.0001$, $P = 0.0002$, respectively). No clinical manifestations differed between the two groups during the disease course, including respiratory failure as well as CNS abnormalities at diagnosis. The proportion of patients who failed VP16 and CSA therapy including HLH94 protocol and needed combination chemotherapy such as CHOP-VP16 before planning SCT was higher in EBV-HLH patients than FHL patients (57% vs. 19%, $P = 0.0168$).

Outcomes of SCT

Engraftment and survival. Post-transplant outcomes of 43 FHL patients and 14 EBV-HLH patients are summarized in Figures 1 and 2. The 10-year OS rates (median ± SE%) of FHL and EBV-HLH patients were 65.0 ± 7.9% and 85.7 ± 9.4%, respectively ($P = 0.24$; Fig. 3). In the allogeneic SCT cases with FHL (Fig. 1), 29 attained engraftment, 6 had rejection or graft failure, and 7 were undetermined. On the other hand, in EBV-HLH (Fig. 2), seven were engrafted, three were rejected, and one was undetermined. Of all 29 FHL patients engrafted after the first SCT, 26 were alive with no HLH relapse, but 3 died of treatment-related mortality (TRM). Seven engrafted patients with EBV-HLH were alive and well at the final follow-up. Among the nine rejection/graft failure patients (six FHL, three EBV-HLH), a second UCBT was successful in three of the four patients (three FHL, one EBV-HLH). Twelve of the UCBT recipients for FHL that received a graft with the first UCBT and two that received a second UCBT were alive at the last follow-up; while seven died; six were due to TRM and one was due to active HLH disease. Six of the seven UCBT recipients for EBV-HLH were alive and well at the last follow-up, while only one died of active HLH disease on day 18 post-transplant. A total of 29 FHL survivors after allogeneic SCT(s) had 17 complete donor chimera (2 patients after second UCBTs), 3 mixed chimera (1 had 42% donor chimera in remission 18 months after SCT, 2 attained >90% donor chimera until 6 months after SCT), 8 undefined, and 1 graft failure with CNS disease. Ten EBV-HLH survivors after allogeneic SCT attained eight complete donor chimera (seven patients after the first SCT and one patient after second SCT [UCBT]), and two with autologous recovery. Two of three EBV-HLH patients who rejected allogeneic cells were alive and disease free more than 6 years post-transplant. One of two EBV-HLH patients who underwent autologous SCT was alive and well 13 years post-transplant [22]. One EBV-HLH patient was alive and well 10 years after the identical twin donor BMT.

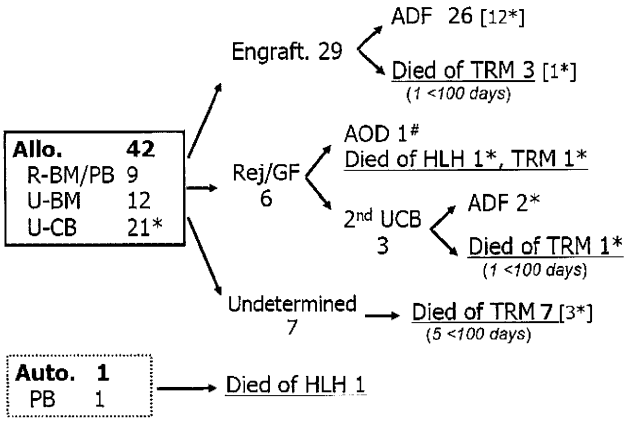

Fig. 1. Cohort diagram for the clinical outcome of 43 patients with familial hemophagocytic lymphohistiocytosis (FHL) who underwent stem cell transplantation (SCT). Of 42 patients after allogeneic SCT, 29 achieved engraftment (18 complete, 3 mixed) and 6 failed to engraft. One (#) with graft failure was alive with central nervous system disease 12 years after SCT. A total of 29 patients (67%) were alive after SCT. The underlined data indicate the number of deceased patients. Seven patients died within 100 days post-SCT (parenthesis). Asterisk (*) means UCB. R, related; U, unrelated; BM, bone marrow; PB, peripheral blood; CB, cord blood; ADF, alive with the disease free state; AOD, alive on disease; Rej/GF, rejection or graft failure; TRM, treatment-related mortality.

Causes of death. Of 14 deceased FHL patients, 12 died of TRM, including 3 chronic GVHD while 2 died of recurrent HLH. Seven patients experienced early death from TRM within 100 days after SCT (Fig. 1). One patient, later diagnosed with FHL2, died of CNS disease 5 years after autologous SCT [14]. Two EBV-HLH patients died of recurrent HLH within 50 days after SCT (Fig. 1). No TRM-related deaths were noted among the EBV-HLH patients.

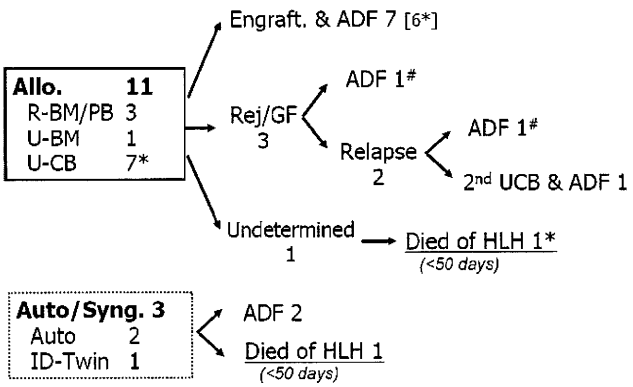

Fig. 2. Cohort diagram for the clinical outcome of 14 patients with Epstein–Barr virus-associated hemophagocytic lymphohistiocytosis (EBV-HLH) who underwent SCT. Among 11 patients after the first allogeneic SCT, 7 achieved successful engraftment and 3 failed to engraft. A total of 12 patients (86%) were alive after SCT. Two patients (#) were alive and well more than 6 years after SCT failure. The underlined data indicate the number of deceased patients. Two patients died within 50 days post-SCT (parenthesis). Asterisk (*) means UCB. Auto/Syng: autologous/syngeneic, ID: identical.

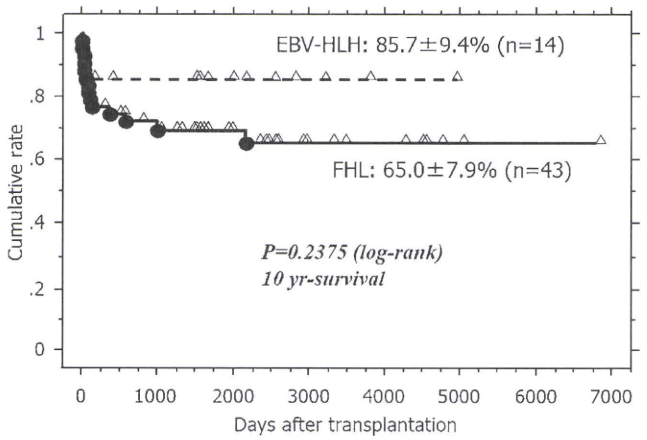

Fig. 3. Cumulative probability of post-transplant overall survival of FHL (*solid line*) and EBV-HLH patients (*dashed line*) who underwent SCT. Closed circle and open triangle represent deceased and alive patients, respectively. Each value indicates the 10-year overall survival rate plus or minus standard error assessed by the log-rank test.

Analysis of Prognostic Factors in FHL

A log-rank test on the OS rate did not show any significant difference in terms of age at SCT (<2 years vs. ≥2 years), time of SCT from HLH treatment (<6 months vs. ≥6 months), conditioning regimens (myeloablative vs. RIC) and various donor sources (R-PB/BM vs. UCBT vs. UBM; Table II). The Cox hazard model with adjustment for gender and age at engraftment indicated that the risk of death for UBM might be higher than that for R-PB/BM (adjusted hazard ratio = 0.07, 95% confidence interval [CI] = 0.01–1.02, $P = 0.05$) and that for UCB (0.27, 95% CI = 0.07–1.09, $P = 0.07$; Table II). No significant variables were found to predict the risk of early death within 100 days post-transplant, or the risk of neurological sequelae.

CNS Abnormalities and Late Sequelae

Table I shows that the frequency of CNS abnormalities at onset and the time of SCT did not differ between the EBV-HLH and FHL patients. Whereas, post-transplant CNS abnormalities were significantly higher in the FHL patients ($P = 0.0015$). Eleven FHL patients (52%) have had late sequelae including neurological as well as endocrinological problems, in comparison to only one EBV-HLH patient with left hemiparesis ($P = 0.022$). Late sequelae of FHL

TABLE II. Association Variables Influencing on the Risk of Mortality in FHL Patients

(A) Log-rank analysis Variables	No.	Survival (OS %)		*P*-value
Age				
<2 years	30	66.2 ± 8.7		0.56
≥2 years	12	75.0 ± 12.5		
Time from HLH treatment				
<6 months	14	62.9 ± 13.3		0.65
≥6 months	28	71.4 ± 8.5		
Conditioning				
Myeloablative	31	71.0 ± 8.2		0.50
RIC	11	60.6 ± 15.7		
Donor sources				
R-PB/BM, a	9	88.9 ± 10.5	a vs. b	0.22
UCB, b	21	65.6 ± 10.6	a vs c	0.15
UBM, c	12	58.3 ± 14.2	b vs c	0.61
(B) Cox's model analysis Variables	No.	Adjusted hazard ratio	95% CI lower–upper limit	*P*-value
Stem cell source				
Unrelated BM	12	1.00	Reference	
Unrelated CB	21	0.27	0.07–1.09	0.07
Related PB/BM	9	0.07	0.01–1.02	0.05
Conditioning				
Reduced intensity	11	1.00	Reference	
Myeloablative	31	0.48	0.09–2.47	0.38
Radiation				
No	31	1.00	Reference	
Yes	11	0.52	0.11–2.52	0.41
Use of ATG				
No	34	1.00	Reference	
Yes	8	0.91	0.18–4.70	0.91
HLA disparity				
No	28	1.00	Reference	
Yes (>1 locus)	14	2.79	0.75–10.38	0.13

Both analyses (A, B) were performed for 42 FHL patients who underwent the first allogeneic SCT. The Cox model analysis was performed with adjustment for selected variables including sex and age at engraftment.

included psychomotor retardation with or without seizures (n = 5), brain atrophy (n = 1), hearing difficulty (n = 1), short stature (n = 5), and impaired sexual development (n = 1).

DISCUSSION

No underlying immunodeficiency has yet been identified for idiopathic EBV-HLH, which has been recognized to be distinct from familial or inherited disease-related HLH like FHL. However, EBV also acts as a trigger in the development of HLH episodes in FHL patients. Therefore, caution must be exercised in the differentiation of the two types of HLH disease. Strict use of the renewed diagnostic criteria for the registered cases in Japan enabled an analysis of the SCT results of 43 FHL and 14 EBV-HLH patients. The data first revealed a high survival rate in UCBT recipients in either type of HLH, indicating that CB could be preferable BM as the unrelated donor source in SCT for pediatric patients with refractory HLH. In addition, SCT in FHL patients was more problematic than that in EBV-HLH, where it was associated with a high incidence of post-transplant early death rate as well as late sequelae including neurological deficits. The EBV-HLH patients showed no apparent sequelae even if they had CNS involvement at diagnosis.

Information concerning SCT for HLH patients has been accumulated mostly in FHL, but little has been published in EBV-HLH except for sporadic case reports [10,11]. Previously published major studies on SCT in FHL patients are summarized in Table III. Because of the historical changes in the available genetic analyses, supportive care practices, donor sources and conditioning, the pre-2000 studies [23–27] might not be comparable to the current data. Henter et al. [21] showed the improved survival of patients treated with HLH-94 followed by BMT, in which the 3-year post-BMT survival was 62%. Horne et al. [28] noted significant TRM due to venoocclusive disease (VOD) after myeloablative conditioning, and that an active disease status at SCT was associated with a poor prognosis. Ouachee-Chardin et al. [29] reported 59% of OS in a series of 48 patients including 60% of haploidentical SCT, and indicated a high TRM due to VOD associated with young age. Recently, Baker et al. [30] reported that BU/CY/VP16 plus or minus ATG-conditioning provided a cure in 53% of patients after unrelated donor BMT, but a high mortality rate at day 100 (32 of 50 [64%] deceased patients). The present study showed a comparably high OS rate (69%) and similarly high incidence of early death until day 100 (7 of 13 [54%] deaths after allogeneic SCT) in Japan. Probably, the major distinction of the current study from the other reports is a higher usage of UCBT (50%) and RIC (26%). Unfortunately, the combined usage of RIC-UCBT was applied only in eight cases (14%) in this study, which was insufficient to fully evaluate its effectiveness. With regard to RIC-SCT with or without UCBT for FHL, Cooper et al. [31] reported a high disease free survival (75%) in 12 HLH patients (including 5 FHL) who underwent RIC-SCT from matched family/unrelated or haploidentical donor, in which 3 of 9 survivors had mixed chimerism but remain free of disease. The most recent report by Cesaro et al. [32] analyzed 61 cases including an appreciable number of RIC (18%) and UCBT (10%), but did not document the superiority of RIC-UCBT. In the present study, UCBT had a tendency to yield a more favorable outcome than UBMT, although the difference was not statistically significant. FHL infants received SCT early; however the fact that survival of FHL patients who underwent SCT at <2 years of age was not better than later SCT might reflect the difficulty in determining the optimal timing of SCT

TABLE III. Reports on the Clinical Outcome of Patients With HLH Who Underwent Allogeneic Hematopoietic Stem Cell Transplantation

No. pts	Median age at SCT (months)	FH (%)	Major conditioning regimen	Donor	Source	OS (%)	Engraft. (%)	Causes of death	Refs.
9	13	45	Myeloab VP16/BU/CY ±anti-LFA1	MRD/MMRD/haplo	BM	44.0	100	TR, HLH	[24]
29	NR	48	Myeloab NR	MRD/MUD/haplo	BM	66.0	72	TR, HLH	[25]
20	9	30	Myeloab VP16/BU/CY ±ATG	MSD/URD (80%)	BM	45.0	90	TR, HLH	[26]
14	14	36	Myeloab VP16/BU/CY, ATG/BU/CY	MMRD/MUD	BM (T cell depleted)	64.3	65	TR, HLH	[27]
12	18	42	Myeloab VP16/BU/CY	MSD/URD (67%)	BM	100	100	No	[33]
17	NR	NR	Myeloab VP16/BU/CY ±ATG, TBI	MRD/URD/haplo	BM, CB (2), PB, CD34	58.0	94	TR, HLH, lymphoma	[8]
65[a]	13	31	Myeloab VP16/BU/CY ±ATG	MRD/URD/haplo	BM, CB (5), PB, CD34	62.0	89	TR, HLH, AML	[21]
86[a]	13	34	Myeloab VP16/BU/CY ±ATG, TBI	MRD/URD/haplo	BM, CB (7)	64.0	90	TR, HLH, 2nd AML	[28]
48	6	35	Myeloab VP16/BU/CY, ATG/BU/CY	MSD/URD/haplo	BM, PB	58.5	78	HLH	[29]
12	14	17	RIC FLU/MEL ± BUS, FLU/2GyTBI	MRD/URD/haplo	BM, CD34	75.0	100	TR	[31]
91	12	NR	Myeloab VP16/BU/CY ±ATG	URD	BM, PB, CB (9)	45.0	83	TR, HLH	[30]
61	13	20	RIC (18%) VP16 or MEL/BU/CY ±ATG	MRD/MMRD/URD	BM, PB, CB (6)	63.9	78	TR (68%), HLH (27%)	[32]
42	17	55	RIC (26%) VP16/BU/CY ±ATG, TBI	MRD/MMRD/URD	BM, PB, CB (21)	69.0	78	TR (79%), HLH (21%)	Ours

AML, acute myelogeneous leukemia; BM, bone marrow; BU, busulfan; CB, cord blood; CY, cyclophosphamide; FHL, familial hemophagocytic lymphohistiocytosis; FH, family history; FLU, fludarabine; MEL, melphalan; MMRD, HLA-mismatched related donor; MRD, HLA-matched related donor; MSD, HLA-matched sibling donor; MUD, HLA-matched unrelated donor; NR, not recorded; PB, peripheral blood; RIC, reduced intensity conditioning; TBI, total body irradiation; TR, transplantation-related events; URD, unrelated donor; VP16, etoposide. [a]Sixty four of 65 patients studied by Henter et al. [21] were included in 86 patients by Horne et al. [28].

or introducing appropriate RIC regimens in young infants. In UCBT, a major obstacle was thought to be early graft failure, but once engrafted no late graft failure could not be seen [29]. We confirmed this finding in our UCBT cases.

Dürken et al. [33] reported that six HLH patients with CNS disease underwent allogeneic BMT and three of them had no persistent neurological problems after transplant. More recently, SCT is thought to be preferable for FHL patients at the early stage of CNS disease with variable presentation [34,35]. Fludarabine-based RIC has been preferred in SCT for FHL patients in order to reduce late sequelae [36,37]. Since CNS disease itself had no impact on the OS in the current study, but nearly half of the long-term survivors of FHL had late sequelae associated with growth and development, further prospective studies should be focused on how to reduce late sequelae in SCT for FHL patients.

In the treatment of refractory EBV-HLH, no consensus has yet been reached concerning the treatment of patients who fail to respond to the HLH-2004 protocol type immunochemotherapy. Several reports documented that SCT led to a complete remission in such cases [8,10,11,28,38,39]. The present study revealed that use of pre-SCT combination chemotherapy might be associated with a better therapeutic impact on subsequent SCT in patients with EBV-HLH. Furthermore, long-term survival, that is, a probable cure, could be obtained even after autologous SCT [22] or identical twin donor BMT, suggesting that a reconstitution of allogeneic hematopoietic stem cells was not essential in the successful SCT for EBV-HLH patients as described in the autologous PBSCT success for lymphoma-associated HLH [40]. In addition, long-term survival even after graft failure or post-transplant relapse in EBV-HLH patients might suggest the possibility of resetting the adaptive immune response to the virus as postulated in autologous SCT for the treatment of autoimmune diseases [41,42]. Moreover, successful syngeneic SCT may imply that EBV-HLH is not a monogenic disease, since Chen et al. [43] observed that a primary infection of EBV incited HLH in a pair of the twins, but not in the identical twin counterpart. These observations implied that the genetic influence in patients with EBV-HLH might be distinct from that in patients with FHL on precipitating the excessive immune activation. Further prospective studies should therefore be directed toward not only the optimization of UCBT-RIC to improve survival of FHL patients, but to better understanding of the pathological interaction between cytotoxic granule disorders and EBV.

ACKNOWLEDGMENT

We thank all contributors of the Japanese Society of Pediatric Hematology who participate in the treatment of HLH patients (Supplemental Table). This work was supported in part by a Grant-in-Aid for Scientific Research (C) #19591255 (O.S.) from the Ministry of Education, Culture, Sports, Science and Technology of Japan, and a fund of the HLH/LCH Committee in the Japanese Society of Pediatric Hematology. We thank Dr. Brian Thomas Quinn (Associate Professor, Department of Linguistic Environment, Faculty of Languages and Cultures, Kyushu University) for kindly correcting the manuscript.

REFERENCES

1. Janka GE. Familial and acquired hemophagocytic lymphohistiocytosis. Eur J Pediatr 2007;166:95–109.
2. Ishii E, Ohga S, Imashuku S, et al. Nationwide survey of hemophagocytic lymphohistiocytosis in Japan. Int J Hematol 2007;86:58–65.
3. Jordan MB, Hildeman D, Kappler J, et al. An animal model of hemophagocytic lymphohistiocytosis (HLH): $CD8^+$ T cells and interferon gamma are essential for the disorder. Blood 2004;104: 735–743.
4. Billiau AD, Roskams T, Van Damme-Lombaerts R, et al. Macrophage activation syndrome: Characteristic findings on liver biopsy illustrating the key role of activated, IFN-gamma-producing lymphocytes and IL-6- and TNF-alpha-producing macrophages. Blood 2005;105:1648–1651.
5. Ohga S, Nomura A, Takada H, et al. Immunological aspects of Epstein-Barr virus infection. Crit Rev Oncol Hematol 2002;44: 203–215.
6. Imashuku S. Systemic type Epstein-Barr virus-related lymphoproliferative diseases in children and young adults: Challenges for pediatric hemato-oncologists and infectious disease specialists. Pediatr Hematol Oncol 2007;24:563–568.
7. Cho EY, Kim KH, Kim WS, et al. The spectrum of Epstein-Barr virus-associated lymphoproliferative disease in Korea: Incidence of disease entities by age groups. J Korean Med Sci 2008;23:185–192.
8. Kasahara Y, Yachie A, Takei K, et al. Differential cellular targets of Epstein-Barr virus (EBV) infection between acute EBV-associated hemophagocytic lymphohistiocytosis and chronic active EBV infection. Blood 2001;98:1882–1888.
9. Imashuku S, Hibi S, Todo S, et al. Allogeneic hematopoietic stem cell transplantation for patients with hemophagocytic syndrome (HPS) in Japan. Bone Marrow Transplant 1999;23: 569–572.
10. Minegishi M, Ohashi Y, Kumaki S, et al. Successful umbilical cord blood transplantation from an unrelated donor for a patient with Epstein-Barr virus-associated hemophagocytic lymphohistiocytosis. Bone Marrow Transplantat 2001;27:883–886.
11. Toubo T, Suga N, Ohga S, et al. Successful unrelated cord blood transplantation for Epstein-Barr virus-associated lymphoproliferative disease with hemophagocytic syndrome. Int J Hematol 2004;80:458–462.
12. Henter JI, Horne A, Aricó M, et al. HLH-2004: Diagnostic and therapeutic guidelines for hemophagocytic lymphohistiocytosis. Pediatr Blood Cancer 2007;48:124–131.
13. Ishii E, Ueda I, Shirakawa R, et al. Genetic subtypes of familial hemophagocytic lymphohistiocytosis: Correlations with clinical features and cytotoxic T lymphocyte/natural killer cell functions. Blood 2005;105:3442–3448.
14. Suga N, Takada H, Nomura A, et al. Perforin defects of primary hemophagocytic lymphohistiocytosis in Japan. Br J Haematol 2002;116:346–349.
15. Yamamoto K, Ishii E, Sako M, et al. Identification of novel MUN13-14-mutations in familial haemophagocytic lymphohistiocytosis and functional analysis of MUNC13-4-deficient cytotoxic T lymphocytes. J Med Genet 2004;41:763–767.
16. Yamamoto K, Ishii E, Horiuchi H, et al. Mutations of syntaxin 11 and SNAP23 genes as causes of familial hemophagocytic lymphohistiocytosis were not found in Japanese people. J Hum Genet 2005;50:600–603.
17. Ueda I, Ishii E, Morimoto A, et al. Phenotypic heterogeneity of familial hemophagocytic lymphohistiocytosis (FHL) in relation to gene mutational characteristics. Pediatr Blood Cancer 2006;46: 482–488.
18. Ohga S, Nomura A, Takada H, et al. Epstein-Barr virus (EBV) load and cytokine gene expression in activated T cells of chronic active EBV infection. J Infect Dis 2001;183:1–7.

19. Okano M, Kawa K, Kimura H, et al. Proposed guidelines for diagnosing chronic active Epstein-Barr virus infection. Am J Hematol 2005;80:64–69.
20. Henter JI, Aricò M, Egeler RM, et al. HLH-94: A treatment protocol for hemophagocytic lymphohistiocytosis. HLH study Group of the Histiocyte Society. Med Pediatr Oncol 1997;28:342–347.
21. Henter JI, Samuelsson-Horne A, Aricò M, et al. Treatment of hemophagocytic lymphohistiocytosis with HLH-94 immunochemotherapy and bone marrow transplantation. Blood 2002;100: 2367–2373.
22. Ohga S, Nomura A, Kai T, et al. Prolonged resolution of hemophagocytic lymphohistiocytosis after high dose chemotherapy followed by autologous peripheral blood stem cell transplantation. Bone Marrow Transplant 1997;19:633–635.
23. Fischer A, Cerf-Bensussan N, Blanche S, et al. Allogeneic bone marrow transplantation for erythrophagocytic lymphohistiocytosis. J Pediatr 1986;108:267–270.
24. Blanche S, Caniglia M, Girault D, et al. Treatment of hemophagocytic lymphohistiocytosis with chemotherapy and bone marrow transplantation: A single-center study of 22 cases. Blood 1991;78: 51–54.
25. Arico M, Janka G, Fischer A, et al. Hemophagocytic lymphohistiocytosis. Report of 122 children from the International Registry. Leukemia 1996;10:197–203.
26. Baker KS, DeLaat CA, Steinbuch M, et al. Successful correction of hemophagocytic lymphohistiocytosis with related or unrelated bone marrow transplantation. Blood 1997;89:3857–3863.
27. Jabado N, de Graeff-Meeder ER, Cavazzana-Calvo M, et al. Treatment of familial hemophagocytic lymphohistiocytosis with bone marrow transplantation from HLA genetically nonidentical donors. Blood 1997;90:4743–4748.
28. Horne A, Janka G, Maarten Egeler R, et al. Haematopoietic stem cell transplantation in haemophagocytic lymphohistiocytosis. Br J Haematol 2005;129:622–630.
29. Ouachee-Chardin M, Elie C, de Saint Basile G, et al. Hematopoietic stem cell transplantation in hemophagocytic lymphohistiocytosis: A single-center report of 48 patients. Pediatrics 2006; 117:e743–e750.
30. Baker KS, Filipovich AH, Gross TG, et al. Unrelated donor hematopoietic cell transplantation for hemophagocytic lymphohistiocytosis. Bone Marrow Transplant 2008;42:175–180.
31. Cooper N, Rao K, Gilmour K, et al. Stem cell transplantation with reduced-intensity conditioning for hemophagocytic lymphohistiocytosis. Blood 2006;107:1233–1236.
32. Cesaro S, Locatelli F, Lanino E, et al. Hematopoietic stem cell transplantation for hemophagocytic lymphohistiocytosis: A retrospective analysis of data from the Italian Association of Pediatric Hematology Oncology (AIEOP). Haematologica 2008;93:1694–1701.
33. Dürken M, Horstmann M, Bieling P, et al. Improved outcome in haemophagocytic lymphohistiocytosis after bone marrow transplantation from related and unrelated donors: A single-centre experience of 12 patients. Br J Haematol 1999;106:1052–1058.
34. Moshous D, Feyen O, Lankisch P, et al. Primary necrotizing lymphocytic central nervous system vasculitis due to perforin deficiency in a four-year-old girl. Arthritis Rheum 2007;56:995–999.
35. Horne A, Trottestam H, Aricò M, et al. Frequency and spectrum of central nervous system involvement in 193 children with haemophagocytic lymphohistiocytosis. Br J Haematol 2008;140: 327–335.
36. Gonzalez-Llano O, Jaime-Pérez J, Cantu-Rodríguez O, et al. Successful father-to-son stem cell transplantation in a child with hemophagocytic lymphohistiocytosis using a reduced-intensity conditioning regimen. Eur J Haematol 2006;77:341–344.
37. Jordan MB, Filipovich AH. Hematopoietic cell transplantation for hemophagocytic lymphohistiocytosis: A journey of a thousand miles begins with a single (big) step. Bone Marrow Transplant 2008;42:433–437.
38. Imashuku S, Teramura T, Tauchi H, et al. Longitudinal follow-up of patients with Epstein-Barr virus-associated hemophagocytic lymphohistiocytosis. Haematologica 2004;89:183–188.
39. Sato E, Ohga S, Kuroda H, et al. Allogeneic hematopoietic stem cell transplantation for Epstein-Barr virus-associated T/natural killer-cell lymphoproliferative disease in Japan. Am J Hematol 2008;83:721–727.
40. Han AR, Lee HR, Park BB, et al. Lymphoma-associated hemophagocytic syndrome: Clinical features and treatment outcome. Ann Hematol 2007;86:493–498.
41. Arkwright PD, Abinun M, Cant AJ. Autoimmunity in human primary immunodeficiency diseases. Blood 2002;99:2694–2702.
42. Brinkman DM, Jol-van der Zijde CM, ten Dam MM, et al. Resetting the adaptive immune system after autologous stem cell transplantation: Lessons from responses to vaccines. J Clin Immunol 2007;27:647–658.
43. Chen CJ, Ho TY, Lu JJ, et al. Identical twin brothers concordant for Langerhans' cell histiocytosis and discordant for Epstein-Barr virus-associated haemophagocytic syndrome. Eur J Pediatr 2004; 163:536–539.

CLINICAL GENETICS
An International Journal of Genetics, Molecular, and Personalized Medicine

Clin Genet 2010: 78: 575–579
Printed in Singapore. All rights reserved

CLINICAL GENETICS
doi: 10.1111/j.1399-0004.2010.01432.x

Short Report

NEMO mutation as a cause of familial occurrence of Behçet's disease in female patients

Takada H, Nomura A, Ishimura M, Ichiyama M, Ohga S, Hara T. *NEMO* mutation as a cause of familial occurrence of Behçet's disease in female patients.
Clin Genet 2010: 78: 575–579. © John Wiley & Sons A/S, 2010

Behçet's disease is a chronic, relapsing, multisystem inflammatory disease of unknown etiology. Nuclear factor κB (NF-κB) essential modulator (NEMO) that is required for the activation of NF-κB plays an important role in inflammation. To investigate the role of NEMO in the pathogenesis of Behçet's disease, we analyzed *NEMO* gene and its expression pattern in tissues in a family with Behçet's disease. We found a heterozygous mutation (1217A>T, D406V) in a 6-year-old girl and her mother. Skewed X-chromosome inactivation was not observed in the peripheral blood mononuclear cells as well as in oral and intestinal mucosa of the patients. Accordingly, there was a significant proportion of peripheral blood monocytes that did not produce sufficient intracellular tumor necrosis factor-α with the stimulation of lipopolysaccharide. Heterozygous *NEMO* mutation is a cause of familial occurrence of Behçet's disease in female patients.

H Takada, A Nomura, M Ishimura, M Ichiyama, S Ohga and T Hara

Department of Pediatrics, Graduate School of Medical Sciences, Kyushu University, Fukuoka, Japan

Key words: Behçet's disease – nuclear factor κB essential modulator Incontinentia pigmenti – X-linked anhidrotic ectodermal dysplasia with immunodeficiency

Corresponding author: Hidetoshi Takada, Department of Pediatrics, Graduate School of Medical Sciences, Kyushu University, 3-1-1, Maidashi, Higashi-ku, Fukuoka 812-8582, Japan.
Tel.: + 81 92 642 5421;
fax: + 81 92 642 5435;
e-mail:
takadah@pediatr.med.kyushu-u.ac.jp

Received 21 December 2009, revised and accepted for publication 12 March 2010

Nuclear factor κB (NF-κB) essential modulator (NEMO) is required for the activation of the transcription factor NF-κB (1). The *NEMO* gene has been mapped to the chromosome location Xq28 (1). Large genomic rearrangements or amorphic mutations of *NEMO* cause incontinentia pigmenti, a disorder that is usually prenatally lethal in males, and contribute to abnormalities of skin, hair, nails, teeth and central nervous system in female heterozygotes (2). On the other hand, hypomorphic *NEMO* mutations cause X-linked anhidrotic ectodermal dysplasia with immunodeficiency (XL-EDA-ID) in male, characterized by immunodeficiency associated with an impaired development of skin adnexa (hair, sweat glands, and teeth) (3).

Behçet's disease is a chronic, relapsing, multisystem inflammatory disease of unknown etiology characterized by mucocutaneous, ocular, articular, vascular, urogenital, neurological, and gastrointestinal involvements, such as ulcerative colitis and congestive gastritis (4, 5). We found heterozygous *NEMO* mutation in two female patients with Behçet's disease.

Materials and methods

Patient 1 was a 6-year-old girl who suffered from ulcers in oral cavity and perianal area for 7 months. Her elder brother was diagnosed as XL-EDA-ID and died of gastrointestinal bleeding when he was 9 years old. On admission, her skin showed hypopigmented lesions without atrophy in the abdominal area and extremities (Fig. 1a), which had been observed since early infancy. A small ulcer was observed in oral

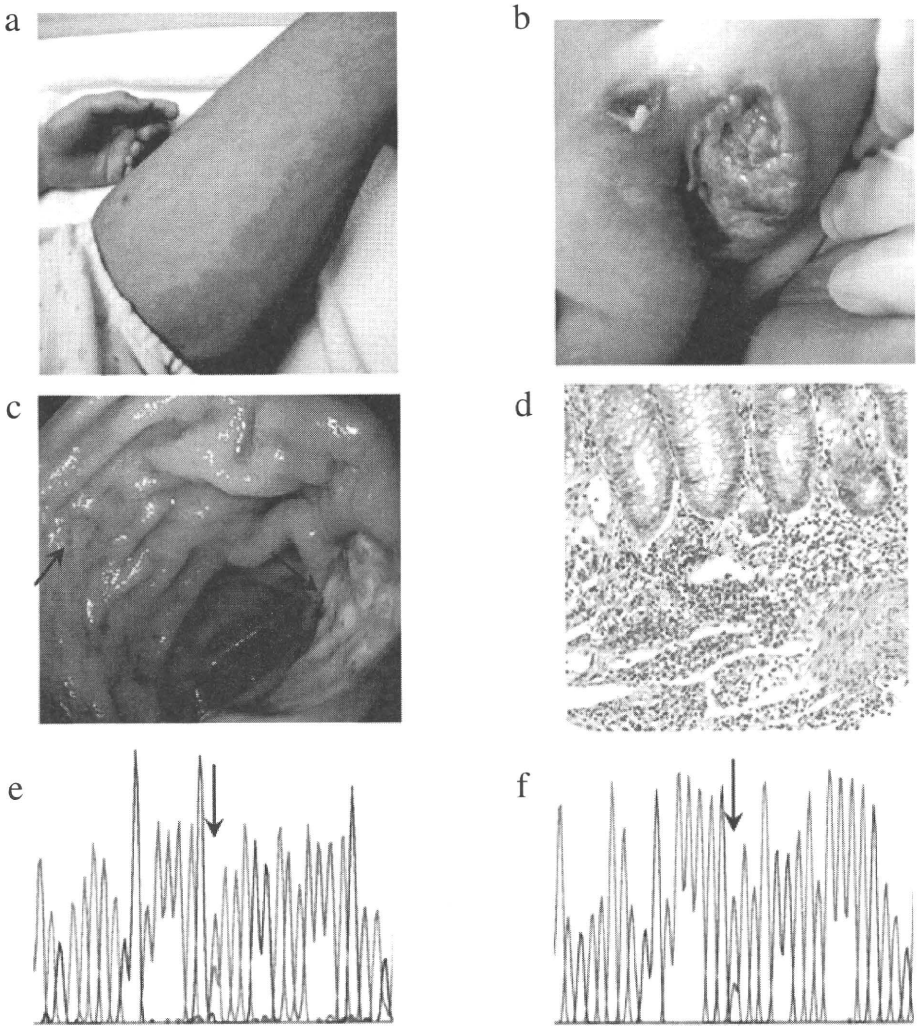

Fig. 1. Clinical manifestations and *NEMO* mutation in the patients. The hypopigmented skin lesions on the lower extremities observed along the curvilinear lines of Blaschko (**a**) and the ulcerative lesions in perianal area (**b**) are shown. The endoscopic finding with ulcerative lesions (arrows) in ascending colon and the histology (hematoxylin–eosin staining, ×100) of the ulcerative lesion are shown in (**c**) and (**d**), respectively. Sequencing results of the peripheral blood cells from patients 1 and 2 on *NEMO* are shown in (**e**; patient 1) and (**f**; patient 2).

cavity. She had large and deep painful ulcerative lesions in perianal area (Fig. 1b). The laboratory examinations showed a white blood cell count of 13.2×10^9/l with 80.9% neutrophils, hemoglobin of 12.3 g/dl, and erythrocyte sedimentation rate of 69 mm/h. Human leukocyte antigen (HLA) typing showed A2/A24, B61/B54, Cw1, Cw15, DR4, and DR12. Endoscopic examination showed multiple ulcerative lesions in colon, lacking reactive change in their marginal area (Fig. 1c). Histologically, chronic active inflammation was observed (Fig. 1d). These findings met the diagnostic criteria for Behçet's disease (entero-Behçet type) (6).

Patient 2 was a 42-year-old mother of the patient 1, who also suffered from ulcers in oral cavity and perianal area since she was 8 years old. She was diagnosed as having Behçet's disease when she was 12 years old. She also had hypopigmented skin lesions in the abdominal area and extremities, which had been observed since early infancy.

Genomic DNA and cDNA were amplified by polymerase chain reaction (PCR) as reported previously (2). The direct sequencing was performed using ABI PRISM 3100 Genetic Analyzer (Perkin-Elmer, Foster City, CA, USA).

Intracellular tumor necrosis factor (TNF)-α staining was performed using the Fastimmune Intracellular Staining System (BD Bioscience Pharmingen, San Diego, CA, USA) (7). Flow cytometric analysis was performed using EPICS XL (Beckman Coulter, Miami, FL, USA).

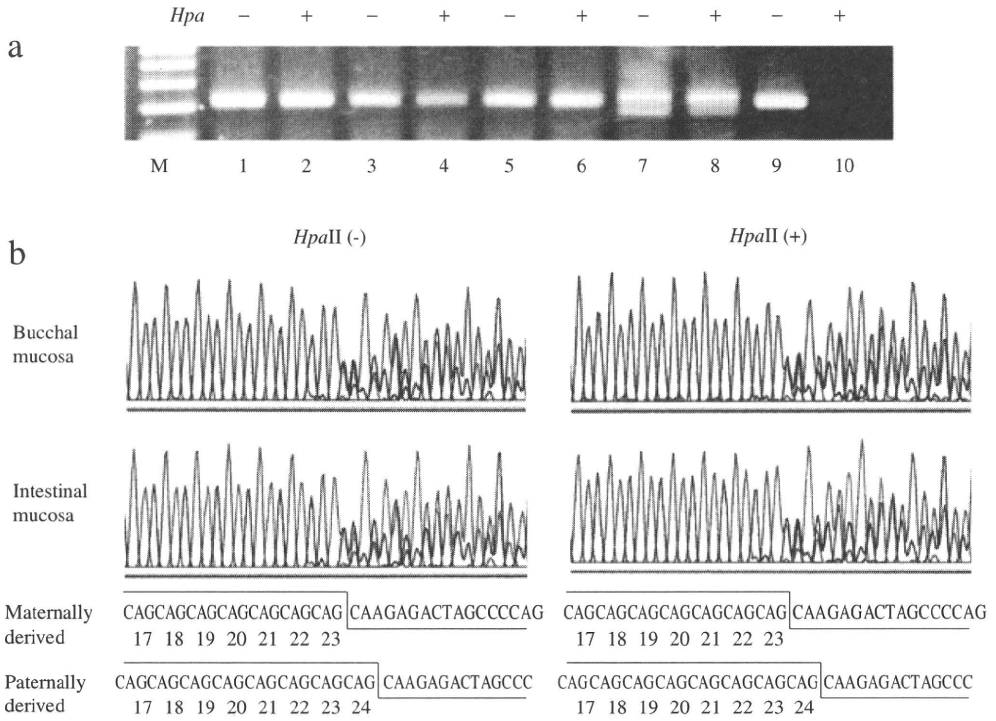

Fig. 2. X-chromosome inactivation of the patients. (**a**) Exon 1 of the HUMARA locus that contains CAG repeats was amplified by PCR after the digestion by methylation-sensitive *Hpa*II. Lanes 1 and 2; PBMNC, lanes 3 and 4; buccal mucosa, lanes 5 and 6; intestinal mucosa of patient 1, lanes 7 and 8; PBMNC of patient 2, lanes 9 and 10; PBMNC of the father of patient 1. (**b**) Sequencing results of the PCR products of the HUMARA locus from PBMNC, and buccal and intestinal mucosa of the patient 1 with and without *Hpa*II treatment are shown. The CAG repeats in the HUMARA locus of the maternally derived and paternally derived X-chromosome were 23 and 24 in number, respectively.

X-chromosome inactivation was analyzed as previously described (8). In brief, DNA was digested with the methylation-sensitive *Hpa*II (New England BioLabs, Beverly, MA, USA), amplified by the PCR at the exon 1 of human androgen receptor (HUMARA) gene locus that contains a highly polymorphic trinucleopeptide repeat (CAG), and sequenced.

Results

The cDNA and genomic DNA were obtained from peripheral blood mononuclear cells (PBMNC), and *NEMO* gene was amplified by PCR and sequenced. Heterozygous mutation (1217A→T, D406V) was observed in patients 1 and 2 (Fig. 1e,f), and elder brother of patient 1 had the same mutation (data not shown). We then investigated X-chromosome inactivation pattern of PBMNC, buccal mucosa, and intestinal mucosa by analyzing the effect of methylation-sensitive *Hpa*II on the HUMARA locus. Although we could not detect the difference of CAG repeat number in HUMARA locus between maternally and paternally derived X-chromosomes by electrophoresis of PCR products due to the minimal (1 repeat) difference in repeat number between them in patient 1 (Fig. 2a), the lack of extreme skewing was confirmed in PBMNC of patient 2 (Fig. 2a). The sequencing of these PCR products showed the lack of extreme skewing in all these tissues in patient 1 (Fig. 2b).

We analyzed lipopolysaccharide (LPS)-induced monocytic TNF-α production using flow cytometer to investigate individual cell function caused by the *NEMO* mutation and X-chromosome inactivation. As shown in Fig. 3, there was a significant proportion of monocytes that did not produce sufficient intracellular TNF-α with the stimulation of LPS, which functionally supported the lack of extensive X-inactivation skewing in the patient.

Discussion

A familial aggregation of Behçet's disease has been reported previously (9–14). Although *Familial Mediterranean fever* (*MEFV*) gene mutation is reported to be one of the genetic backgrounds of Behçet's disease (15), most of the patients as well as our patients did not have *MEFV* mutation (data not shown). There are several

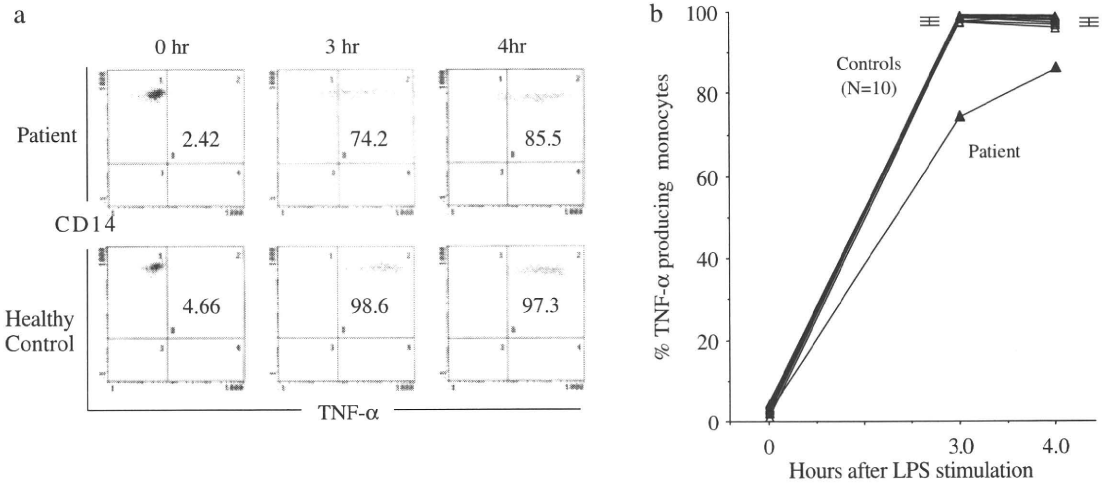

Fig. 3. A population of peripheral blood monocytes with insufficient production of intracellular TNF-α by the stimulation of LPS. A representative data of intracellular TNF-α staining (**a**) and the percentage of TNF-α producing cells in monocytes (**b**) without and with LPS stimulation are shown. Horizontal bars indicate the mean value and standard deviation in healthy controls.

reports of the association of Behçet's disease and incontinentia pigmenti (16–18). All the patients were females and developed Behçet's disease in childhood (16–18), which further supports our results.

Several clinically unique features were observed in our patients. The first was the occurrence of incontinentia pigmenti and XL-EDA-ID in a family. The second was the hypopigmented skin lesions since early infancy, because they are usually observed in early teens to adulthood (19). The third was the lack of extremely skewed X-chromosome inactivation (Fig. 2). Most of the patients with incontinentia pigmenti showed skewed X-chromosome inactivation in PBMNC and hepatocytes, which spared any apparent phenotype of these cells (20). This *NEMO* mutation was reported previously only in one patient with XL-EDA-ID (21), not in females. The D406V mutation locates in zinc finger domain, which is important in phosphorylation of NEMO, binding with ubiquitin, and full NF-κB activation (22–24). The development of Behçet's disease may be restricted only in a small proportion of the patients with incontinentia pigmenti caused by some particular type of *NEMO* mutation. Alternatively, it is possible that there are unrecognized patients with Behçet's disease and atypical or mild skin lesions caused by *NEMO* mutations.

NEMO-deficient mice developed intestinal inflammation by the impaired intestinal integrity caused by increased sensitivity to TNF-induced cell death, diminished expression of antimicrobial peptides such as defensins, and recruitment of inflammatory cells into damaged tissues (25). It is possible that this occurs in female patients with heterozygous *NEMO* mutation if they do not have skewed X-chromosome inactivation in the intestine. Immunocompetent inflammatory cell fraction in these patients can be recruited and it accelerates the inflammatory reaction in the intestine. The latter seems to be more important for the development of the Behçet's disease, because low-dose corticosteroid treatment was effective in both patients. This mechanism would also be applied to the lesions in oral mucosa and perianal tissues where continuous bacterial stimulation and infection occur.

Acknowledgements

This work was supported by a grant for Research on Intractable Diseases from the Ministry of Health, Labour and Welfare of Japan, and a Grant-in Aid for Scientific Research to H. T. from the Ministry of Education, Science, Sports, and Culture of Japan.

Conflict of interest

Nothing to declare.

References

1. Yamaoka S, Courtois G, Bessia C et al. Complementation cloning of NEMO, a component of the IkappaB kinase complex essential for NF-kappaB activation. Cell 1998: 93: 1231–1240.
2. Smahi A, Courtois G, Vabres P et al. Genomic rearrangement in NEMO impairs NF-kappaB activation and is a cause of incontinentia pigmenti. The International Incontinentia Pigmenti (IP) Consortium. Nature 2000: 405: 466–472.
3. Zonana J, Elder ME, Schneider LC et al. A novel X-linked disorder of immune deficiency and hypohidrotic ectodermal dysplasia is allelic to incontinentia pigmenti and due to

mutations in IKK-gamma (NEMO). Am J Hum Genet 2000: 67: 1555–1562.
4. Chajek T, Fainaru M. Behçet's disease. Report of 41 cases and a review of the literature. Medicine 1975: 54: 179–196.
5. Koné-Paut I, Yurdakul S, Bahabri SA et al. Clinical features of Behçet's disease in children: an international collaborative study of 86 cases. J Pediatr 1998: 132: 721–725.
6. The Behçet's Disease Research Committee of Japan. Skin hypersensitivity to streptococcal antigens and the induction of systemic symptoms by the antigens in Behçet's disease: a multicenter study. J Rheumatol 1989: 16: 506–511.
7. Takada H, Yoshikawa H, Imaizumi M et al. Delayed separation of the umbilical cord in two siblings with Interleukin-1 receptor-associated kinase 4 deficiency: rapid screening by flow cytometer. J Pediatr 2006: 148: 546–548.
8. Takada H, Kanegane H, Nomura A et al. Female agammaglobulinemia due to the Bruton tyrosine kinase deficiency caused by extremely skewed X-chromosome inactivation. Blood 2004: 103: 185–187.
9. Dündar SV, Gençalp U, Simşek H. Familial cases of Behçet's disease. Br J Dermatol 1985: 113: 319–321.
10. Akpolat T, Koc Y, Yeniay I et al. Familial Behçet's disease. Eur J Med 1992: 1: 391–395.
11. Nishiura K, Kotake S, Ichiishi A et al. Familial occurrence of Behçet's disease. Jpn J Ophthalmol 1996: 40: 255–259.
12. Kone-Paut I, Geisler I, Wechsler B et al. Familial aggregation in Behçet's disease: high frequency in siblings and parents of pediatric probands. J Pediatr 1999: 135: 89–93.
13. Gül A, Inanç M, Ocal L et al. Familial aggregation of Behçet's disease in Turkey. Ann Rheum Dis 2000: 59: 622–625.
14. Fietta P. Behçet's disease: familial clustering and immunogenetics. Clin Exp Rheumatol 2005: 23: S96–S105.
15. Touitou I, Magne X, Molinari N et al. MEFV mutations in Behçet's disease. Hum Mutat 2000: 16: 271–272.
16. Ammann AJ, Johnson A, Fyfe GA et al. Behçet syndrome. J Pediatr 1985: 107: 41–43.
17. Menni S, Piccinno R, Biolchini A et al. Incontinentia pigmenti and Behcet's syndrome: an unusual combination. Acta Derm Venereol 1986: 66: 351–354.
18. Endoh M, Yokozeki H, Maruyama R et al. Incontinentia pigmenti and Behçet's disease: a case of impaired neutrophil chemotaxis. Dermatology 1996: 192: 285–287.
19. Berlin AL, Paller AS, Chan LS. Incontinentia pigmenti: a review and update on the molecular basis of pathophysiology. J Am Acad Dermatol 2002: 47: 169–187.
20. Nelson DL. NEMO, NFkappaB signaling and incontinentia pigmenti. Curr Opin Genet Dev 2006: 16: 282–288.
21. Jain A, Ma CA, Liu S et al. Specific missense mutations in NEMO result in hyper-IgM syndrome with hypohydrotic ectodermal dysplasia. Nat Immunol 2001: 2: 223–228.
22. Carter RS, Pennington KN, Ungurait BJ et al. In vivo identification of inducible phosphoacceptors in the IKKγ/NEMO subunit of human IκB kinase. J Biol Chem 2003; 278: 19642–19648.
23. Cordier F, Grubisha O, Traincard F et al. The zinc finger of NEMO is a functional ubiquitin-binding domain. J Biol Chem 2009: 284: 2902–2907.
24. Shifera AS, Horwits M. Mutations in the zinc finger domain of IKKγ block the activation of NF-κB and the induction of IL-2 in stimulated T lymphocytes. Mol Immunol 2008: 45: 1633–1645.
25. Nenci A, Becker C, Wullaert A et al. Epithelial NEMO links innate immunity to chronic intestinal inflammation. Nature 2007: 446: 557–561.

THE JOURNAL OF IMMUNOLOGY

Smad2 and Smad3 Are Redundantly Essential for the TGF- β–Mediated Regulation of Regulatory T Plasticity and Th1 Development

Tomohito Takimoto, Yu Wakabayashi, Takashi Sekiya, Naoko Inoue, Rimpei Morita, Kenji Ichiyama, Reiko Takahashi, Mayako Asakawa, Go Muto, Tomoaki Mori, Eiichi Hasegawa, Saika Shizuya, Toshiro Hara, Masatoshi Nomura and Akihiko Yoshimura

J Immunol 2010;185;842-855; Prepublished online 14 June 2010;
doi:10.4049/jimmunol.0904100
http://www.jimmunol.org/content/185/2/842

The Journal of Immunology is published twice each month by
The American Association of Immunologists, Inc.,
9650 Rockville Pike, Bethesda, MD 20814-3994.

Print ISSN: 0022-1767 Online ISSN: 1550-6606.

Smad2 and Smad3 Are Redundantly Essential for the TGF-β–Mediated Regulation of Regulatory T Plasticity and Th1 Development

Tomohito Takimoto,*,† Yu Wakabayashi,* Takashi Sekiya,* Naoko Inoue,* Rimpei Morita,* Kenji Ichiyama,* Reiko Takahashi,* Mayako Asakawa,* Go Muto,* Tomoaki Mori,* Eiichi Hasegawa,* Saika Shizuya,‡ Toshiro Hara,† Masatoshi Nomura,† and Akihiko Yoshimura*,§

Although it has been well established that TGF-β plays a pivotal role in immune regulation, the roles of its downstream transcription factors, Smad2 and Smad3, have not been fully clarified. Specifically, the function of Smad2 in the immune system has not been investigated because of the embryonic lethality of Smad2-deficient mice. In this study, we generated T cell-specific *Smad2* conditional knockout (KO) mice and unexpectedly found that Smad2 and Smad3 were redundantly essential for TGF-β–mediated induction of Foxp3-expressing regulatory T cells and suppression of IFN-γ production in $CD4^+$ T cells. Consistent with these observations, *Smad2/Smad3*-double KO mice, but not single KO mice, developed fatal inflammatory diseases with higher IFN-γ production and reduced Foxp3 expression in $CD4^+$ T cells at the periphery. Although it has been suggested that Foxp3 induction might underlie TGF-β–mediated immunosuppression, TGF-β still can suppress Th1 cell development in Foxp3-deficient T cells, suggesting that the Smad2/3 pathway inhibits Th1 cell development with Foxp3-independent mechanisms. We also found that Th17 cell development was reduced in Smad-deficient $CD4^+$ T cells because of higher production of Th17-inhibotory cytokines from these T cells. However, TGF-β–mediated induction of RORγt, a master regulator of Th17 cell, was independent of both Smad2 and Smad3, suggesting that TGF-β regulates Th17 development through Smad2/3-dependent and -independent mechanisms. *The Journal of Immunology*, **2010, 185: 842–855.**

Among the three TGF-β isoforms, TGF-β1 is predominantly expressed in the immune system and is an important pleiotropic cytokine with potent immunoregulatory properties (1, 2). Mice deficient in TGF-β1 develop a multiorgan autoimmune inflammatory disease and die a few weeks after birth (3, 4). Various transgenic mice whose T cells are unable to respond specifically to TGF-β1 have also been shown to develop autoimmunity, indicating that TGF-β1 signaling is essential for T cell homeostasis (5–7).

Various mechanisms have been proposed for the immunoregulatory functions of TGF-β on T cells, such as suppression of cell proliferation, cytokine production, and cytokine signaling, as well as inducing apoptosis (8). TGF-β has been shown to induce Foxp3 (9), a master transcriptional factor of regulatory T cells (Tregs) (10, 11). The overexpression of Foxp3 in $CD4^+$ T cells suppressed the production of proinflammatory cytokines, including IL-2, IFN-γ, IL-4, and IL-17 (12–14). Foxp3 is predominantly expressed in thymus-derived, naturally occurring Tregs, which are critically important for immunoregulation (15). Likewise, in vitro TGF-β–induced Tregs (iTregs) can suppress effector T cell proliferation in vitro and autoimmune diseases in vivo, just as nTregs can (16). Furthermore, TGF-β signaling has been reported to be essential for the maintenance of nTregs at the periphery and for their development in the thymus (17).

The major signaling pathways of the TGF-βRs are relatively simple (18). TGF-β first binds to the TGF-βR, which then mainly activates Smad transcription factors, including three structurally similar proteins, two receptor-associated Smads, Smad2 and Smad3, and one common Smad4. Smad2 or Smad3 are directly phosphorylated and activated by TGF-βR and heterodimerize with Smad4 or TIF1γ (19). The activated Smad-complex translocates into the nucleus and, in a cooperative manner with other nuclear cofactors, regulates the transcription of target genes.

Many previous reports have indicated that TGF-β is required to orchestrate T cell immunity, but it is not clear whether various TGF-β–mediated effects on T cells are equally dependent on Smad signaling. It has been reported that Smad2 or Smad3 regulates a distinctive set of genes in fibroblasts and tumor cells (18). *Smad2*-knockout (KO) mice are embryonic-lethal (20) and *Smad3*-KO mice exhibit inflammatory diseases (21), suggesting that Smad2 is involved in mediating signals during development, whereas Smad3 is important for anti-inflammation. A recent

*Department of Microbiology and Immunology, Keio University School of Medicine, Shinjyuku-ku; §Japan Science and Technology Agency, Core Research for Evolutional Science and Technology, Chiyoda-ku, Tokyo; †Graduate School of Medical Sciences, Kyushu University, Fukuoka; and ‡Department of Ophthalmology, Wakayama Medical University School of Medicine, Wakayama, Japan

Received for publication December 22, 2009. Accepted for publication May 3, 2010.

This work was supported by Grants-in-Aid for Scientific Research and for Scientific Research on Priority Areas from the Ministry of Education, Culture, Sports, Science and Technology of Japan; the Program for Promotion of Fundamental Studies in Health Sciences of the National Institute of Biomedical Innovation; the Naito Foundation; the Mochida Foundation; and the Astellas Foundation for Research on Metabolic Disorders.

Address correspondence and reprint requests to Dr. Akihiko Yoshimura, Department of Microbiology and Immunology, Keio University School of Medicine, 35 Shinanomachi, Shinjuku-ku, Tokyo, 160-8582, Japan. E-mail address: yoshimura@a6.keio.jp

The online version of this article contains supplemental material.

Abbreviations used in this paper: DKO, double knockout; EAE, experimental autoimmune encephalomyelitis; iTreg, in vitro TGF-β–induced Treg cell; KO, knockout; MLN, mesenteric lymph node; MOG, myelin oligodendrocyte glycoprotein; Treg, regulatory T cell.

www.jimmunol.org/cgi/doi/10.4049/jimmunol.0904100

report suggested that Smad3, but not Smad2, is critical for the induction of Foxp3 (22). Moreover, the disruption of Smad4 specifically in T cells results in colitis and an increased susceptibility to the spontaneous colo-rectal tumorigenesis (23). These reports might indicate that the Smad3/4 pathway is an important mediator of TGF-β signaling in immune regulation. However, the phenotypes of Smad3- or Smad4-deficient mice were much milder than those of T cell-specific *TGF-βRII* KO mice (7), suggesting that Smad2 may also play a role in immune regulation.

Because *Smad2* completely-null mice were embryonic-lethal, the roles of Smad2 in the immune system have not been clarified; one question that remains open is whether Smad2 and Smad3 have any overlapping and/or specific functions in vivo. To address these questions, we generated T cell-specific *Smad2* conditional KO mice. Our study also revealed unexpected overlapping functions of Smad2 and Smad3 in the regulation of various T cell responses and gene expressions. Our data indicated that Smad3 and Smad2 are important for TGF-β–mediated Foxp3 induction and suppression of Th1 development. We also found that Th17 cell development was indirectly regulated by Smad2/3 signaling. Furthermore, we found that TGF-β suppressed Th1 cell development in a Foxp3-independent manner. These data suggest that the TGF-β/Smad pathway regulates T cell responses via multiple mechanisms.

Materials and Methods

Mice

Construction of the *Smad2-flox* vector and generation of the *Smad2*$^{f/f}$ mice will be described elsewhere (M. Nomura, manuscript in preparation). LckCre mice with a C57BL/6 background (24) expressing Cre recombinase under the control of the mouse proximal *Lck* gene were crossed with *Smad2*$^{f/f}$ mice. Offspring carrying both *LckCre* and floxed *Smad2* genes were used for intercrossing and further analysis. Littermates without the LckCre allele (*Smad2*$^{f/f}$) were used as control mice for analysis purposes. *Smad3* KO mice with a C57BL/6 background were provided by Dr. Flanders (National Institutes of Health, Bethesda, MD) (25). Nomenclature of genotypes of Smad2/Smad3 KO mice and T cells is listed in Table I. *Scurfy* mice (C57BL/6) have been described elsewhere. Age- and sex-matched littermates were used as control mice in all experiments. Genotypes were determined by PCR, using the following primer pairs: 5′-TGAGACTTCTCTGTACCCGAT-3′ and 5′-CATCAGATTCCATTAGAGATGG-3′. Mice were kept in specific pathogen-free facilities in Keio University. All experiments using mice were approved by and performed according to the guidelines of the Animal Ethics Committee of Keio University.

T cell isolation and differentiation

$CD4^+CD25^-CD44^{low}CD62L^{high}$ naive T cells or $CD4^+CD25^{high}CD44^{low}CD62L^{high}$ nTregs from spleens and lymph nodes and also, in some cultures, from thymi were enriched by negative selection using the magnetic cell sorting system (Miltenyi Biotec, Auburn, CA) with biotin-conjugated anti-CD8.2 (53-6.7), anti-B220/CD44 (RA3-6B2), anti-CD11b (M1/70), anti-CD11c (N418), anti-TER119, and anti-NK1.1 (PK136) Abs (eBioscience, San Diego, CA) as well as streptoavidin-conjugated magnetic beads (Miltenyi Biotec). Cells were then FACS-sorted using a BD FACS aria cell sorter (BD Biosciences, San Jose, CA). The purity of the sorted $CD4^+$ T cell populations was consistently >98%. T cells were activated by anti-CD3e (145-2C11) and anti-CD28 (37.51) and cultured in the presence of recombinant murine IL-12 (10 ng/ml; PeproTech, Rocky Hill, NK) and anti–IL-4 (5 μg/ml; 11B11) for Th1 cell differentiation; recombinant murine IL-4 (10 ng/ml; PeproTech) and anti–IFN-γ (5 μg/ml, R4-6A2) for Th2 cell differentiation; recombinant hTGF-β1 (2 ng/ml; R&D Systems, Minneapolis, MN), anti–IFN-γ (5 μg/ml), and anti–IL-4 (5 μg/ml) for Treg differentiation; and recombinant human TGF-β1 (0.5 ng/ml), recombinant human IL-6 (20 ng/ml; R&D Systems), anti–IFN-γ (5 μg/ml), and anti–IL-4 (5 μg/ml) for Th17 cell differentiation (26, 27). In some cultures, for induction of Th17 cells, anti–IL-2 (10 μg/ml; 1A12, eBioscience) was added. T cells were maintained in a complete medium containing RPMI 1640 supplemented with 10% FCS, 1% penicillin/streptomycin, 100 nM non-essential amino acids, 2mM glutamine, and 0.05 mM 2-ME.

Western blot analysis

Cells were washed, lysed in sample buffer, and boiled. Whole cell lysates were separated by SDS-PAGE under reducing conditions and transferred to a polyvinylidene difluoride membrane (Millipore, Bedford, MA) as described elsewhere (28). The membrane was blocked and probed with the following primary Abs: anti–β-actin rabbit polyclonal Ab (A2066; Sigma-Aldrich, St. Louis, MO) and anti-Smad2/3 rabbit mAb (#3102, Cell Signaling Technology, Beverly, MA). The membrane was then probed with appropriate secondary Abs conjugated to HRP and visualized with the ECL Detection System (GE Healthcare, Tokyo, Japan), according to the manufacturer's instructions. β-Actin was used as a loading control.

Flow cytometry

For intracellular cytokine staining, cells were stimulated for 6 h in complete medium with phorbol 12-myristate 13-acetate (50 ng/ml) and ionomycin (500 ng/ml; both from Sigma-Aldrich) in the presence of brefeldin A (eBioscience). Surface staining was then performed in the presence of Fc-blocking Abs (2.4G2), followed by intracellular staining for cytokines with the Fixation and Permiabilization kit (eBioscience) according to the manufacturer's protocol. All Abs were from eBioscience. For intracellular staining of Foxp3, the Foxp3-Staining Buffer Set (fixation/permeabilization and permeabilization buffers, eBioscience) was used according to the manufacturer's protocol. Data were acquired on a BD FACS aria and were analyzed with FlowJo software (Tree Star, Ashland, OR).

ELISA

Supernatants were collected after the indicated periods of cell culture and were analyzed for IL-2, IFN-γ, IL-4, and IL-17A with an ELISA kit (eBioscience) according to the manufacturer's protocol.

Real-time RT-PCR

cDNA was synthesized and analyzed by real-time quantitative PCR as described previously (29). Gene expression was examined with a Bio-Rad iCycler Optical System with the iQ SYBR green real-time PCR kit (Bio-Rad, Hercules, CA). The data were normalized to HPRT. The primers have been described previously (29). The relative expression of the indicated gene to HPRT was calculated as $(2^{-[\text{experimental CT} - \text{HPRT CT}]}) \times 1000$, where *CT* is the cycle threshold of signal detection.

CFSE labeling and suppression assay

For CFSE labeling, sorted naive $CD4^+$ T cells were washed twice with HBSS (Invitrogen), and labeled with 5 mM CFSE (Sigma-Aldrich) in HBSS for 10 min at 20°C. The labeling was then stopped by adding 1/5 volume of FCS. The labeled cells were washed twice with the T cell culture medium before they were seeded and stimulated as described in the text. $CD4^+CD25^{high}CD44^{low}CD62L^{high}$ nTregs from *Smad2*$^{f/f}$ mice or LckCre-*Smad2*$^{f/f}$ mice were FACS-sorted (purity >98%), as were naive $CD4^+$ T cells as responder cells. Naive $CD4^+$ T cells (1×10^5 cells) and the indicated number of nTregs were cultured with irradiated splenocytes (3×10^4 cells) with 2 μg/ml anti-CD3e Ab for 3 d. CFSE dilution was analyzed on a BD Biosciences FACS Aria.

Microarrays

RNA was prepared from 3×10^6 cells of stimulated cells as described previously (28). Total RNA was cleaned with RNeasy Micro Kit (QIAGEN). Microarray processing was done by the Central Research Laboratory, School of Medicine, Keio University on a fee-for-service basis according to the recommendations in the Affymetrix GeneChip Expression Analysis Technical Manual (Affymetrix, Santa Clara, CA). The cRNA was hybridized to M430 2.0 microarray chips (Affymetrix). Hybridized chips were stained and washed and were scanned with a GeneArray scanner 3000 7G (Affymetrix). GeneSpring software (Tomy, Tokyo, Japan) was used for comparison analyses. Microarray data are deposited in the National Center for Biotechnology Information GEO database. (www.ncbi.nlm.nih.gov/geo/query/acc.cgi?token=zpotpcgkcyqauhg&acc=GSE19601)

Experimental autoimmune encephalomyelitis induction

Myelin oligodendrocyte glycoprotein (MOG) peptide 35–55 (MEVGWYRSPFSRVVHLYRNGK) (BEX) was used to induce experimental autoimmune encephalomyelitis (EAE) in mice (30, 31). Mice were injected s.c. with 200 μg of MOG peptide in 100 μl of PBS emulsified in 100 μl CFA that was further enriched with 5 mg/ml *Mycobacterium tuberculosis* (H37Ra; Difco BD Biosciences). In addition, 500 ng pertussis toxin (Calbiochem, San Diego, CA) was injected i.p. on days 0 and 2. Paralysis was evaluated according to the following scores: 0, no signs; 1, full tail; 2, hind limbs; 3, complete back; 4, forelimbs; 5, dead.

Statistics

A paired Student *t* test was used to determine statistical significance, and $p < 0.05$ was considered significant. Error bars show standard deviations.

Results

Generation of Smad2 conditional KO mice

To clarify the role of Smad2 in immune regulation, we generated T cell-specific *Smad2*-conditional KO mice. We first generated mice carrying a modified *Smad2* allele in which exon 7 and exon 8 were flanked by *lox*P sites (floxed). There was no difference between C57BL/6 wild-type mice and $Smad2^{f/fl}$ control mice in T cell development, nTreg functions in vitro, and $CD4^+$ T cell responses to TGF-β (Supplemental Fig. 1) (data not shown). We then deleted *Smad2* specifically in T cells by crossing $Smad2^{f/f}$ mice with LckCre transgenic mice, in which Cre recombinase was driven by the *Lck* promoter (LckCre). Smad2 protein was undetectable in naive $CD4^+$T cells isolated from LckCre-$Smad2^{f/f}$ (*Smad2*-cKO) mice (Fig. 1*A*). The resulting *Smad2*-cKO mice were fertile and were born with the expected Mendelian frequency (data not shown). *Smad2*-cKO mice appeared healthy and had no evident signs of autoimmunity, but a small fraction (<5%) of aged *Smad2*-cKO mice spontaneously developed inflammatory bowel diseases (data not shown). Moreover, *Smad2*-cKO mice were much more susceptible to dextran sodium sulfate induced colitis,

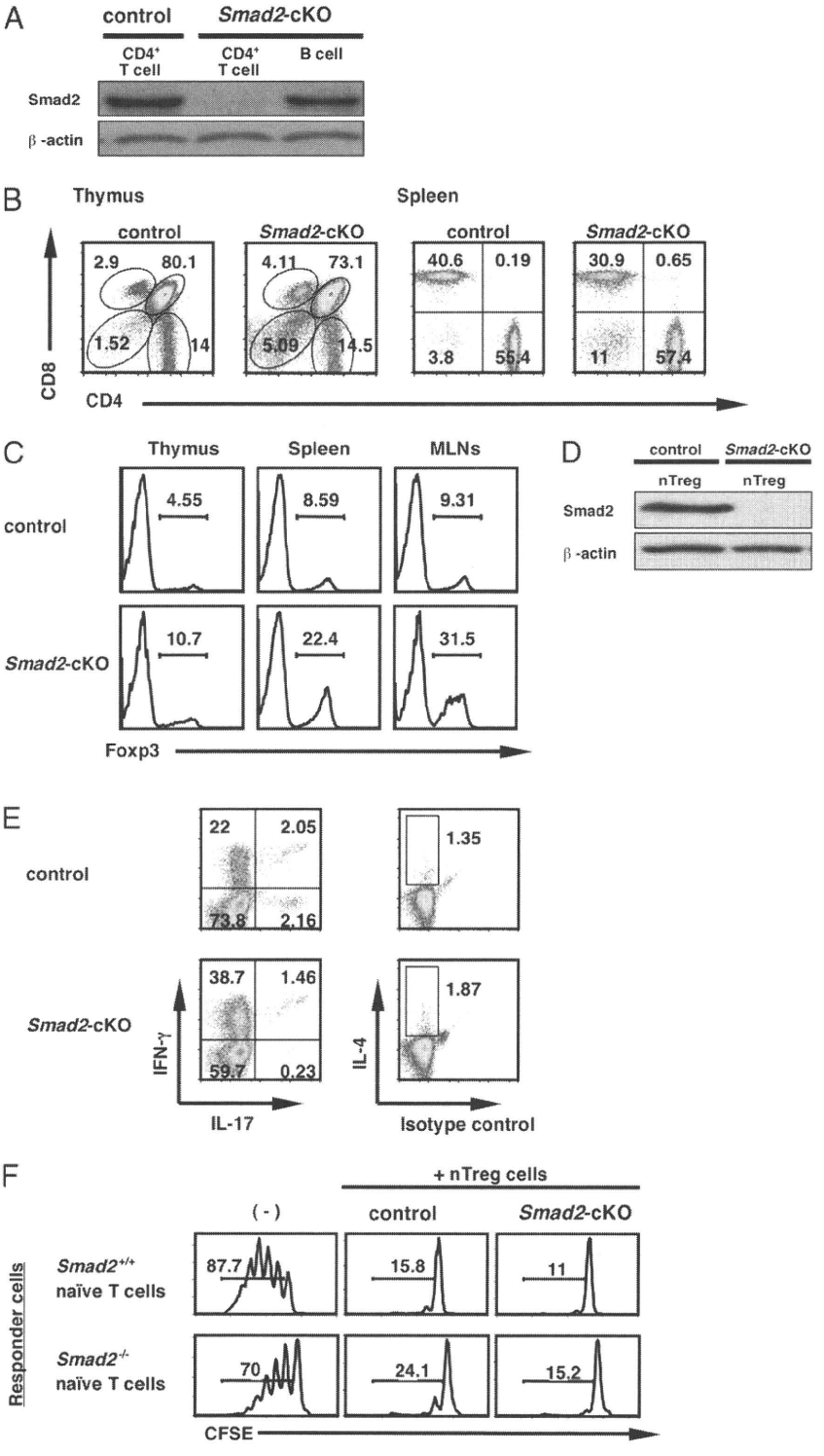

FIGURE 1. T cell-specific deletion of *Smad2* abrogates T cell homeostasis in vivo. *A*, Immunoblot of lysates of FACS-sorted $CD4^+$ $CD25^-CD44^{low}CD62L^{high}$ T cells (naive T cells) isolated from $Smad2^{f/f}$ (control) or LckCre-$Smad2^{f/f}$ (*Smad2*-cKO) mice (loading control: β-actin). Data shown are representative of two independent experiments on different mice. *B*, Flow cytometry of freshly isolated T cells from thymus and spleen in control and *Smad2*-cKO mice at 8 wk old. Five mice per group were analyzed with similar results. *C*, Flow cytometry of freshly isolated $CD4^+$ T cells from thymus, spleen, and MLNs in indicated mice at 8 wk old. Cells were fixed and stained for intracellular Foxp3. Histograms are gated on CD4-single-positive subsets. Five mice per group were analyzed with consistent results. *D*, Immunoblot of lysates of FACS-sorted $CD4^+CD25^{high}CD44^{low}CD62L^{high}$ nTregs isolated from control or *Smad2*-cKO mice (loading control: β-actin). Data shown are representative of two independent experiments on different mice with similar results. *E*, Flow cytometry of freshly isolated CD4+ T cells from spleen in indicated mice at 8 mo old. Cells were stimulated for 5 h with PMA and ionomycin. Brefeldin A was added to cultures before 1 h. Cells were assessed for the indicated cytokine expression by intracellular staining. Data shown are representative of five mice per group. *F*, CFSE-labeled naive $CD4^+$ T cells from control or *Smad2*-cKO mice were cultured with or without $CD4^+$ $CD25^{high}CD44^{low}CD62L^{high}$ nTregs from control or *Smad2*-cKO mice in triplicate wells with irradiated splenocytes and stimulated with 2 μg/ml of anti-CD3 Abs for 3 d. Proliferation was estimated by CFSE dilution. Each histogram was gated on a CD4-positive subset. Representative data of two independent experiments are shown. MLNs, mesenteric lymph nodes.

which is deteriorated by IFN-γ (32), than were control littermates (data not shown). These observations suggest that *Smad2*-cKO mice were more sensitive to inflammatory stress than control ($Smad2^{f/fl}$) littermate mice were.

Characterization of Smad2-deficient T cells

First, we characterized T cells in *Smad2*-cKO mice. The development of T cells in the thymus and spleen were normal in *Smad2*-cKO mice (Fig. 1*B*). As was found to be true of *Smad3*-KO mice (33), *Smad2*-cKO mice can also generate nTregs, and the fraction of nTregs in the indicated organs was 2- to 3-fold higher in *Smad2*-cKO mice than in control littermate mice (Fig. 1*C*). We confirmed that Smad2 protein was also undetectable in nTregs isolated from *Smad2*-cKO mice (Fig. 1*D*). Peripheral $CD4^+$ T cells from *Smad2*-cKO mice produced more IFN-γ, but less IL-17, after stimulation with PMA and ionomycin (Fig. 1*E*). IL-4 levels were not found to be significantly different. These activated phenotypes of $CD4^+$ T cells in *Smad2*-cKO were not due to nTreg dysfunction, because nTregs from *Smad2*-cKO mice ($Smad2^{-/-}$ in Fig. 1*F*) showed a sufficient suppressive function, equivalent to that seen in nTregs from control mice ($Smad2^{+/+}$ in Fig. 1*F*). Naive $Smad2^{-/-}$ $CD4^+$ T cells also showed similar sensitivity to the suppressive effect of nTregs (Supplemental Fig. 2).

Phenotypes of LckCre-Smad2 $^{f/f}$Smad3$^{-/-}$ mice

Then we generated *Smad2* and *Smad3* double KO (DKO) mice by crossing *Smad2*-cKO mice and $Smad3^{-/-}$ (*Smad3*-KO) mice to compare T cell phenotypes among Smad2-cKO, Smad3-KO and *Smad2/3*-DKO mice. To understand the genotype easier, description of genotypes of T cells and mice is listed in Table I.

Overall, $CD4^+$ T cell phenotypes of *Smad2*-cKO mice resembled those of *Smad3*-KO mice (Fig. 2) (21). Although Smad2 signaling seems to be important in T cells, as we demonstrated above, the phenotypes of *Smad2*-cKO mice and those of *Smad3*-KO mice were much milder than those of *TGF-β1*–KO mice (4) or T cell-specific *TGF-βRII*–cKO mice (7). Whereas *Smad2/3*-DKO mice showed severe inflammation and died within 3–5 wk (Fig. 2*A–C*). Severe atrophy of the thymus was observed, and the total number of T cells in the thymus was extremely reduced (Fig. 2*D*). The population of activated–memory phenotype with $CD25^+CD44^{high}$ $CD62L^{low}$ was increased in peripheral $CD4^+$ T cells isolated from Smad2-cKO mice but not from Smad3-KO mice (Fig. 2*E*). Most of the peripheral $CD4^+$ T cells in *Smad2/3*-DKO mice showed an activated memory phenotype (Fig. 2*E*). The fraction of Foxp3-expressing cells in the thymus of *Smad2/3*-DKO mice was similar to that of littermate control ($Smad2^{fl/fl}Smad3^{+/+}$) mice, whereas Foxp3-expressing cells in the periphery of these mice were severely reduced (Fig. 2*F*). These results suggested that TGF-β–Smad signaling was not always necessary for the generation of nTregs in vivo. These phenotypes of *Smad2/3*-DKO mice were similar to those of T cell-specific *TGF-βRII*–cKO mice, suggesting that the immunosuppressive functions of Smad2 and Smad3 overlap each other and are redundantly essential for TGF-β signaling in T cells.

The compatible roles of Smad2 and Smad3 in regulating the gene transcription by TGF-β

It has been shown that, unlike Smad3, Smad2 lacks a DNA-binding domain; therefore, Smad2 has been suggested to regulate different genes than does Smad3 (18). However, the functions of Smad2 and Smad3 in gene regulation of T cells have not been investigated. To investigate the requirement of Smad2 or Smad3 for TGF-β–mediated gene regulation, we performed a microarray analysis. We used TGF-β1 in all experiments because TGF-β1 is believed to be the major TGF-β involved in immune regulation. Because *Smad2/3*-DKO mice had too low a number of naive $CD4^+$ T cells as shown in Fig. 2*E*, we used $Smad2^{-/-}Smad3^{+/-}$ $CD4^+$ T cells from LckCre-$Smad2^{f/f}$/$Smad3^{+/-}$ (2cKO/3hetero) mice for microarray analysis. A similar approach was performed previously to identify Smad2 and Smad3 common target genes in keratinocytes (34). We considered that $Smad2^{-/-}Smad3^{+/-}$ $CD4^+$ T cells were still useful to identify Smad2/3-dependent and -independent genes, because Foxp3 induction by TGF-β was severely impaired in $Smad2^{-/-}$ $Smad3^{+/-}$ T cells (Supplemental Fig. 3).

Naive $CD4^+$ T cells from control, *Smad2*-cKO, *Smad3*-KO, or 2cKO/3hetero mice were stimulated with anti-CD3e/CD28 with or without TGF-β for 24 h. We compared genes upregulated >4-fold and downregulated <0.25-fold by TGF-β in $Smad2^{+/+}Smad3^{+/+}$ $CD4^+$ T cells. A significant number of genes were regulated by Smad2 and Smad3 specifically (8% was Smad2-specific and 20% was Smad3-specific). However, the role of these genes in T cells has not been clarified. We found that a large proportion of TGF-β–regulated genes were both Smad2 and Smad3-dependent (Smad2/3-dependent); 64% (increase) and 90% (decrease) of genes, including *Foxp3, Ahr, IRF8, Ikzf4 (Eos), c-maf* (up), and *IL-2* (down), were equally affected by either Smad2 or Smad3 deficiency (Fig. 3*A*, 3*B*, Supplemental Fig. 4). These data suggested that not only Smad3 but also Smad2 were required in TGF-β–mediated transcriptional regulation in T cells. Notably, most of the Treg signature genes (35, 36) were similarly affected by Smad2 or Smad3 deficiency (Fig. 3*C*).

Interestingly, we found several TGF-β–regulated genes that which were not affected by Smad2/3-deficiency, including *RORγt, CD73, Ccr8, Socs2* (up), and *eomes* (down). These data collectively indicated that TGF-β organizes the gene transcription in T cells through both a Smad2/3-dependent and -independent manner; however, most TGF-β–inducible genes involved in T cell functions and differentiation are shown to be common targets of Smad2 and Smad3.

Induction and maintenance of Foxp3 by TGF-β were redundantly dependent on Smad2 and Smad3

Next, we confirmed the involvement of Smad signaling in iTreg differentiation by TGF-β. As shown in Fig. 4*A*, when cultured in the presence of TGF-β and IL-2, Foxp3 mRNA expression levels

Table I. *Description of the genotypes used in this study*

T Cell		Mouse	
Control	$Samd2^{fl/fl}Smad3^{+/+}$	Control	$Samd2^{fl/fl}Smad3^{+/+}$
$Samd2^{-/-}Smad3^{+/+}$	$Samd2^{del/del}Smad3^{+/+}$	Smad2-cKO	LckCre$Smad2^{fl/fl}Smad3^{+/+}$
$Samd2^{-/-}Smad3^{-/-}$	$Samd2^{fl/fl}Smad3^{-/-}$	Smad3-KO	$Smad2^{fl/fl}Smad3^{-/-}$
$Samd2^{-/-}Smad3^{+/-}$	$Samd2^{del/del}Smad3^{+/-}$	2cKO/3hetero	LckCre$Smad2^{fl/fl}Smad3^{+/-}$
$Samd2^{-/-}Smad3^{-/-}$	$Samd2^{del/del}Smad3^{-/-}$	2/3-DKO	LckCre$Smad2^{fl/fl}Smad3$

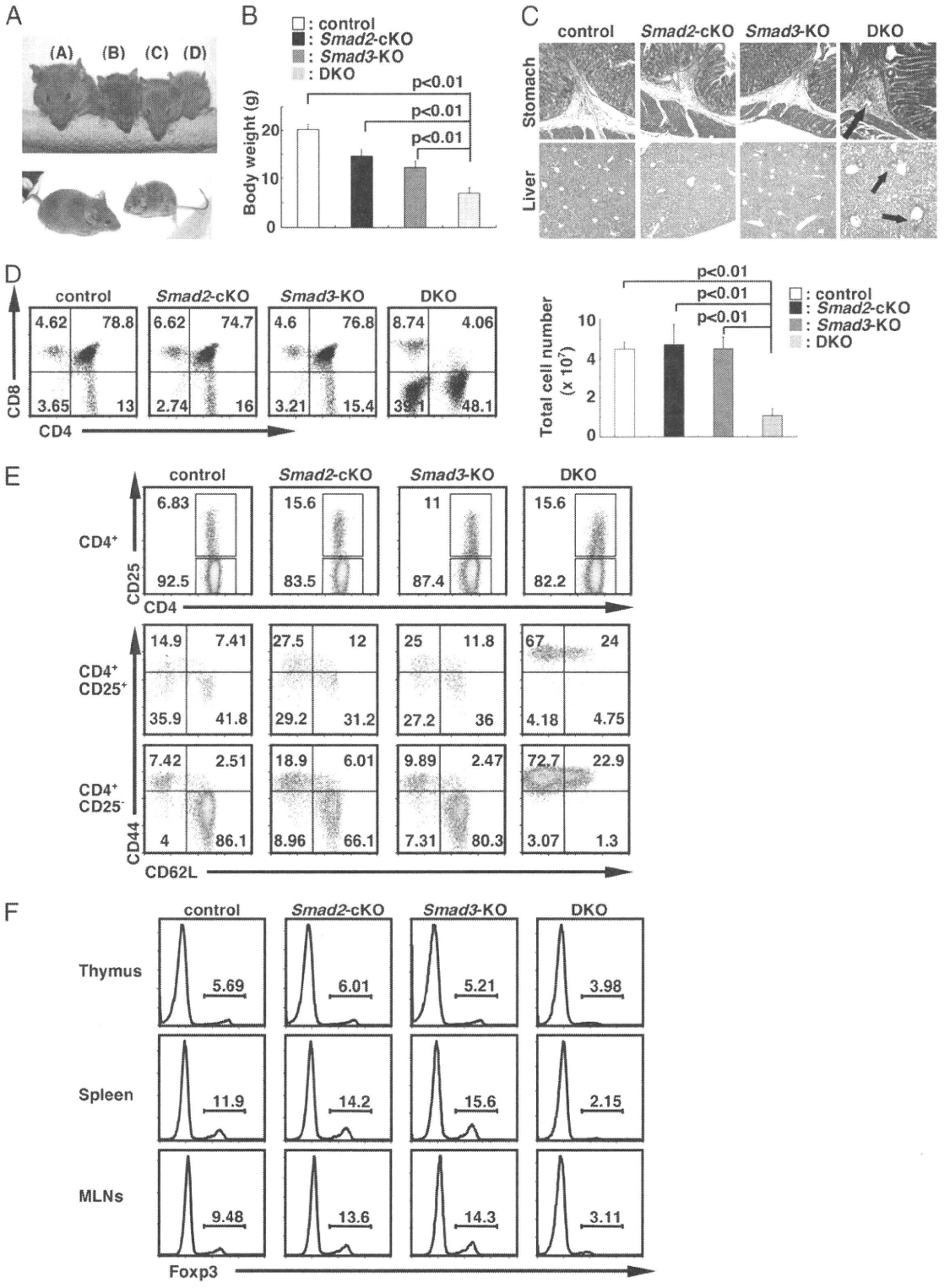

FIGURE 2. The genetic ablation of both Smad2 and Smad3 in T cells causes severe inflammatory diseases. Appearance of LckCre-*Smad2*$^{f/f}$*Smad3*$^{-/-}$ (DKO) mice. The left panel shows, from left to right, the front image of (*A*) control (*Smad2*$^{f/f}$*Smad3*$^{+/+}$), (*B*) *Smad2*-cKO (LckCre-*Smad2*$^{f/f}$*Smad3*$^{+/+}$), (*C*) *Smad3*-KO (*Smad2*$^{f/f}$*Smad3*$^{-/-}$), and (*D*) DKO (LckCre-*Smad2*$^{f/f}$*Smad3*$^{-/-}$) mice, respectively. All mice were 4-wk-old male littermates. The *right panel* shows lateral images of mice; *left*, control (*Smad2*$^{f/f}$*Smad3*$^{+/+}$) and *right*, *Smad2/3*-DKO (LckCre-*Smad2*$^{f/f}$*Smad3*$^{-/-}$). A bar graph shows the mean body weights of *Smad2*$^{f/f}$*Smad3*$^{+/+}$ (control; $n = 15$), LckCre-*Smad2*$^{f/f}$*Smad3*$^{+/+}$ (*Smad2*-cKO; $n = 13$), *Smad2*$^{f/f}$*Smad3*$^{-/-}$ (*Smad3*-KO; $n = 12$) and LckCre-*Smad2*$^{f/f}$*Smad3*$^{-/-}$ (DKO; $n = 10$) mice at the age of 4 wk. Statistical differences were verified by paired Student *t* test. Histologic analysis by H&E staining of indicated organs from indicated mice at 4 wk old (original magnification ×20). Black arrows indicate inflammatory cell infiltration. Data shown are representative from one of the five tissue samples with similar results. *D*, CD4/CD8 profile of freshly isolated CD3$^+$ T cells from the thymus of indicated mice at 4 wk old. A bar graph shows the mean total cell number of thymocytes. *E*, Expression of activation–memory markers on freshly isolated CD4$^+$ T cells from spleens of indicated mice at 4 wk old. *Upper*, *middle*, and *lower panels* are gated on CD4–single-positive, CD4$^+$CD25$^+$ and CD4$^+$CD25$^-$ subsets, respectively. Ten mice per group were analyzed and representative data are shown. *F*, Foxp3 expression in freshly isolated CD4$^+$ T cells from

were partially decreased in *Smad2*$^{-/-}$*Smad3*$^{+/+}$ CD4$^+$ T cells and *Smad2*$^{+/+}$*Smad3*$^{-/-}$ CD4$^+$T cells. Reduced iTreg differentiation of *Smad2*$^{-/-}$*Smad3*$^{+/+}$ CD4$^+$ T cells was confirmed by Foxp3 immunostaining (Fig. 4*B*). In the absence of Smad2, the iTreg fraction was rapidly decreased after day 4 in culture (Fig. 4*B*).

Foxp3 induction was markedly reduced in *Smad2*$^{-/-}$*Smad3*$^{+/-}$ CD4$^+$T cells. Furthermore, TGF-β never induced Foxp3 mRNA in naive *Smad2*$^{-/-}$*Smad3*$^{-/-}$ CD4$^+$ T cells (Fig. 4*A*), which was consistent with microarray data (Fig. 3*A*). These data indicate that TGF-β–mediated Foxp3 induction is completely dependent on Smad signaling. In addition, one Smad in Foxp3 induction can partly compensate for the loss of another Smad.

Previous reports have suggested that TGF-β could also be involved in the maintenance of Foxp3 expression in nTregs at the periphery (7, 17); however, the role of Smad signaling has not been identified. We isolated CD4$^+$CD25^{high}CD44^{low}CD62L^{high} T cells as nTregs by FACS (>98% Foxp3-positive day 0) (Fig. 4*C*). The fraction of Foxp3-positive cells was decreased to 44% in *Smad2*$^{+/+}$*Smad3*$^{+/+}$ nTregs in the absence of TGF-β, and TGF-β partly maintained their Foxp3 expression to 61% (Fig. 4*C*, *top row*). *Smad2*$^{-/-}$*Smad3*$^{+/+}$ or *Smad2*$^{+/+}$*Smad3*$^{-/-}$ nTregs lost their Foxp3 expression more intensively than did *Smad2*$^{+/+}$*Smad3*$^{+/+}$ nTregs within this in vitro culture period, but TGF-β still increased the levels of Foxp3 in these cells (Fig. 4*C*, *middle two rows*). However, *Smad2*$^{-/-}$*Smad3*$^{+/-}$ nTregs lost Foxp3 expression more profoundly, and TGF-β showed little effect on Foxp3 maintenance in these cells (Fig. 4*C*, *bottom row*). We also observed that Smad2-deficient nTregs more rapidly lost their Foxp3 expression in vivo, when transferred into *Rag2*$^{-/-}$ mice (Supplemental Fig. 5). These data suggest that TGF-β is involved in the maintenance of Foxp3 in nTregs via a Smad2 and Smad3-dependent mechanism.

TGF-β–mediated suppression of Th1 cell differentiation was dependent on both Smad2 and Smad3

It has been shown that TGF-β strongly inhibits Th1 cell differentiation from naive CD4$^+$ T cells (37). Furthermore, Foxp3 in CD4$^+$ T cells has been shown to suppress the production of various cytokines, including IFN-γ. To clarify the role of Smad2 and Smad3 in TGF-β–mediated suppression of Th1 cell differentiation, and its relationship to Foxp3 induction, we compared Th1/iTreg differentiation among *Smad2*$^{+/+}$*Smad3*$^{+/+}$, *Smad2*$^{-/-}$*Smad3*$^{+/+}$, *Smad2*$^{+/+}$*Smad3*$^{-/-}$, or *Smad2*$^{-/-}$*Smad3*$^{+/-}$ CD4$^+$ T cells. Naive CD4$^+$ T cells were cultured in the Th1-skewing condition in the presence of various concentrations of TGF-β. As shown in Fig. 5*A* and 5*B*, in control *Smad2*$^{+/+}$*Smad3*$^{+/+}$ cells, TGF-β efficiently suppressed generation of IFN-γ–producing cells, but strongly induced Foxp3-positive cells. Th1 cell development was partially suppressed in *Smad2*$^{-/-}$*Smad3*$^{+/+}$ or *Smad2*$^{+/+}$*Smad3*$^{-/-}$ CD4$^+$ T cells by TGF-β at the concentration where Foxp3 induction was partially impaired. Moreover, the suppression of Th1 cell development and Foxp3 induction was barely observed in *Smad2*$^{-/-}$*Smad3*$^{+/-}$ CD4$^+$ T cells at any concentrations of TGF-β. These data indicate that TGF-β–mediated Th1 suppression and iTreg induction were strictly dependent on Smad2/3 signaling. The data in Fig. 5*B* suggest an inverse correlation between Th1 suppression and Foxp3 induction.

TGF-β–mediated CD103 induction was Smad2/3-dependent

The $\alpha_E\beta_7$ integrin is a cell surface receptor that interacts with E-cadherin on epithelial cells (38). The α_E subunit, CD103 is expressed on immune cells, including CD8$^+$ T cells, Tregs, and dendritic cells, and CD103$^+$ cells can accumulate in nonlymphoid tissues expressing E-cadherin. In addition, CD103 in Tregs has been implicated in suppressive activity (39). Because TGF-β also has been reported to upregulate CD103 expression in CD4$^+$ T cells (38), we examined the role of Smad signaling in CD103 expression by TGF-β (Fig. 5*C*). Induction of CD103 by TGF-β occurred mainly in Foxp3$^+$ T cells in *Smad2*$^{+/+}$*Smad3*$^{+/+}$ CD4$^+$ T cells. TGF-β–mediated expression of CD103 was dependent on Smad2/3 signaling, because almost no induction of CD103 was observed in *Smad2*$^{-/-}$*Smad3*$^{+/-}$ T cells. Interestingly, *Smad2*$^{+/+}$*Smad3*$^{-/-}$ and *Smad2*$^{-/-}$*Smad3*$^{+/+}$ CD4$^+$ T cells expressed low levels of CD103, even in Foxp3$^+$ cells (compare Fig. 5*A*, 5*C*). These data suggest that CD103 induction by TGF-β was more strictly dependent on Smad2 or Smad3 than Foxp3 induction.

TGF-β suppresses Th1 cell differentiation by Foxp3-independent mechanisms

Because Foxp3$^+$ cells barely produced IFN-γ (12), the above data suggested that Foxp3 induction by TGF-β in naive CD4$^+$ T cells could be the most important mechanism in TGF-β–mediated regulation of Th1 cell differentiation.

To verify this possibility, we used Foxp3-deficient T cells from *scurfy* mice, which have a nonfunctioning mutant *Foxp3* gene allele (40). Unexpectedly, TGF-β sufficiently inhibited Foxp3-deficient CD4$^+$ T cells from differentiating into Th1 cells, just as it did in wild-type CD4$^+$ T cells (Fig. 6*A*, 6*B*). Next, we examined whether TGF-β could also regulate Th1 cell differentiation in a Foxp3-independent manner in vivo. We administered recombinant TGF-β into *scurfy* mice on a daily basis. It is well known that *scurfy* mice develop fatal autoimmune diseases, and that various cytokines secreted by excessively activated CD4$^+$ T cells play an important role in their pathologies (40, 41). Notably, exogenously administered TGF-β efficiently suppressed severe autoimmune phenotypes of *scurfy* mice (Fig. 6*C*, 6*D*). Microscopic studies showed milder tissue destruction and inflammatory cell infiltration in the livers of TGF-β–treated *scurfy* mice than in those of PBS-treated *scurfy* mice (Fig. 6*D*). Consistent with these results, CD4$^+$ T cells isolated from lymph nodes or spleens of TGF-β–treated *scurfy* mice showed lower production levels of IL-2, IFN-γ, and IL-4 than did those from PBS-treated *scurfy* mice (Fig. 6*E*) (data not shown). These observations indicate that TGF-β can suppress the responses of CD4$^+$ T cells without inducing Foxp3.

Smad2/3 signaling is required for effective Th17 cell development, but not for the induction of RORγt

Recent studies have shown that TGF-β acts as an inducer of IL-17–producing Th17 cells in mice and humans, especially when combined with proinflammatory cytokines, such as IL-6 or IL-21 (42–44). Th17 cells are now accepted as one of the main causes of the pathogenesis of various murine autoimmune diseases including EAE (30). First, we examined the effect of Smad2 deficinecy in T cells on EAE. As shown in Fig. 7*A* and 7*B*, the clinical features associated with the EAE model were milder in *Smad2*-cKO mice than in control littermate mice. The level of IL-17 production from CD4$^+$ T cells in diseased *Smad2*-cKO mice was lower than those from the control littermate mice. These data suggest that Smad2 positively regulates Th17 cell differentiation (Fig. 7*C*). However, CD4$^+$ T cells in *Smad2*-cKO mice produced higher levels of IFN-γ or IL-2 than did those in the control

thymi, spleens, and MLNs of indicated mice at 4 wk old. Cells were fixed and stained for intracellular Foxp3. Data are representative of five independent experiments with similar results. MLNs, mesenteric lymph nodes.

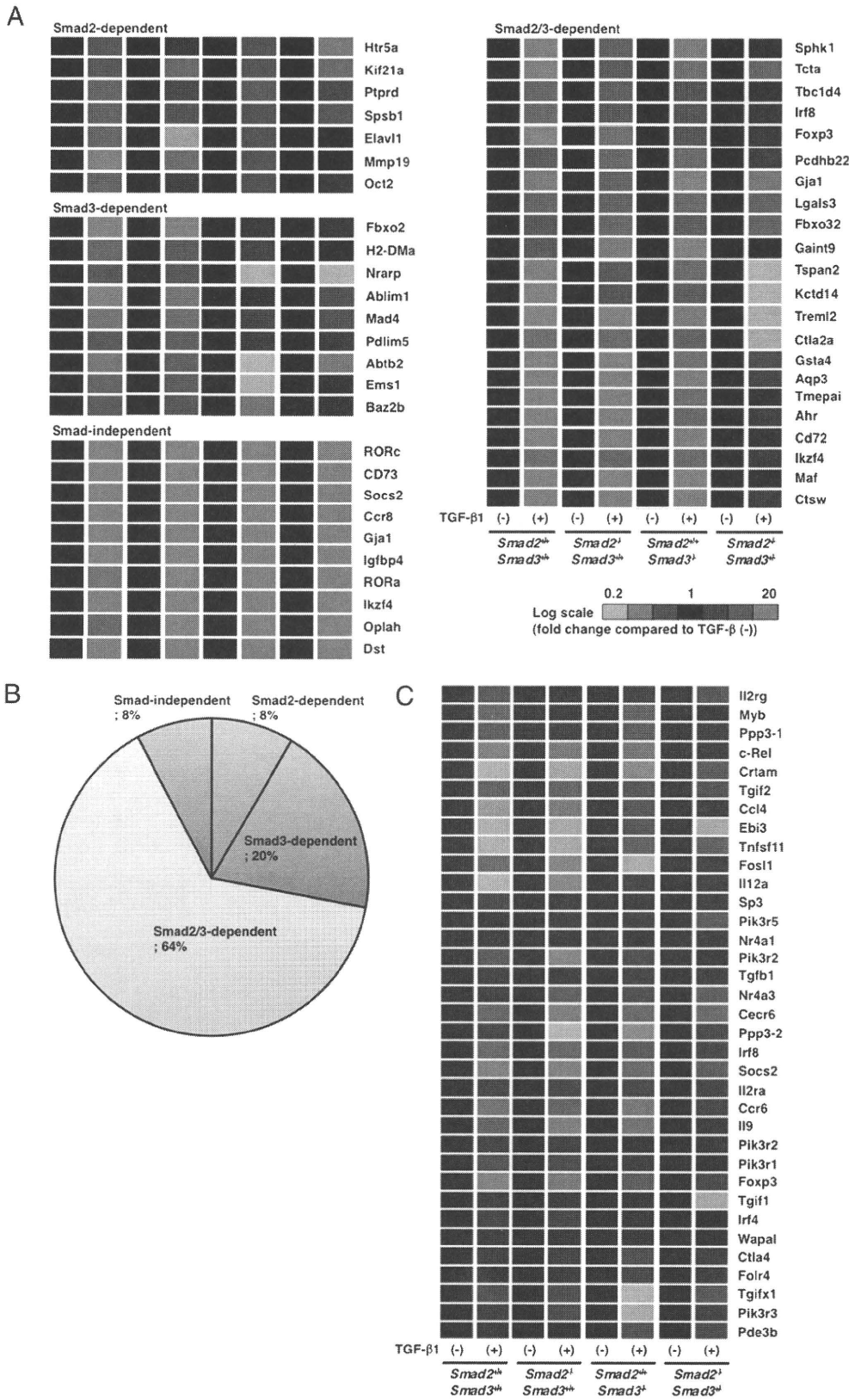

FIGURE 3. Microarray analysis of TGF-β-regulated genes in CD4$^+$ T cells. *A*, Fold change comparing the effect of TGF-β on CD4$^+$ T cells in gene expression. FACS-sorted naive CD4$^+$ T cells cells from control (*Smad2*$^{+/+}$*Smad3*$^{+/+}$), *Smad2*-cKO (*Smad2*$^{-/-}$*Smad3*$^{+/+}$), *Smad3*-KO (*Smad2*$^{+/+}$*Smad3*$^{-/-}$), and 2cKO/3hetero (*Smad2*$^{-/-}$*Smad3*$^{+/-}$) mice were stimulated by anti-CD3e/CD28 and IL-2 with or without 2ng/ml of TGF-β1 in the presence of anti-IFN-γ and anti-IL-4 for 24 h. Genes upregualted >4-fold by TGF-β1 in *Smad2*$^{+/+}$*Smad3*$^{+/+}$ CD4$^+$ T cells were compared. Levels of upregulated genes by TGF-β1 in indicated cells were compared with the same genotype cells stimulated without TGF-β, normalized as 1 of the expression value. Transcriptional profiling of indicated cells was performed using Affymetrix M430 2.0 microarrays. *B*, Relationship between Smad-dependent and Smad-independent genes revealed by expression array analysis in upregulated genes by TGF-β. *C*, Same comparison of fold change as in *A*, with the Treg signature genes.

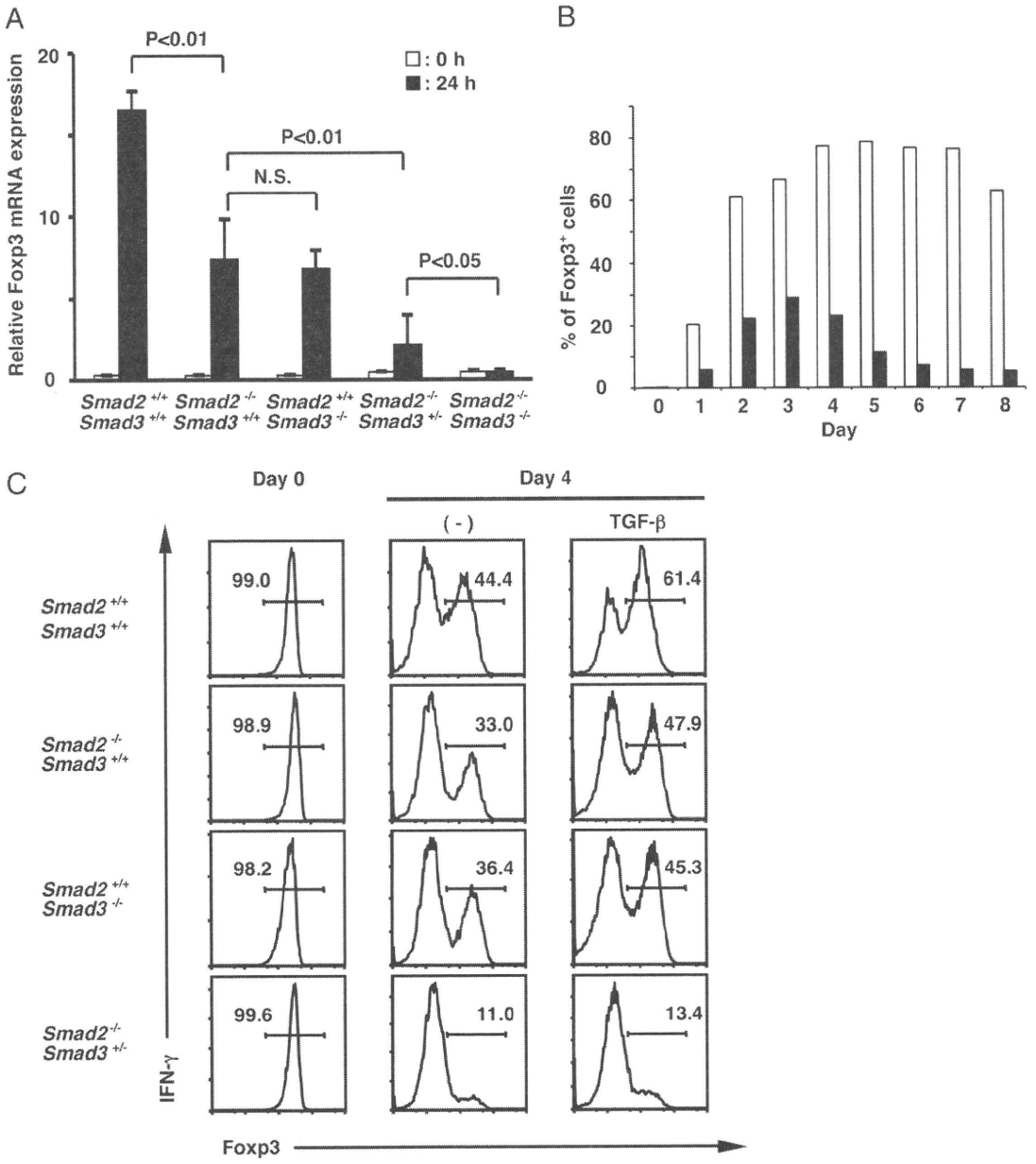

FIGURE 4. TGF-β–mediated induction and maintenance of Foxp3 in Smad2- and Smad3- deficient T cells. *A*, FACS-sorted naive CD4$^+$ T cells from control (*Smad2*$^{+/+}$*Smad3*$^{+/+}$), *Smad2*-cKO (*Smad2*$^{-/-}$*Smad3*$^{+/+}$), *Smad3*-KO (*Smad2*$^{+/+}$*Smad3*$^{-/-}$), 2cKO/3hetero (*Smad2*$^{-/-}$*Smad3*$^{+/-}$), and DKO (*Smad2*$^{-/-}$*Smad3*$^{-/-}$) mice were stimulated under the Treg-skewing condition for 24 h. At 0 and 24 h, mRNA expression of Foxp3 was assessed by real-time RT-PCR. The experiment was performed in duplicate. Data shown were normalized to the expression of a reference gene, *HPRT*. The expression for *Foxp3* gene of *Smad2*$^{+/+}$*Smad3*$^{+/+}$ CD4$^+$ T cells at 0 h was set as 1. Bars show means ± SD. Data are representative of two independent experiments with consistent results. Statistical differences were verified by paired Student *t* test. *B*, FACS-sorted *Smad2*$^{+/+}$*Smad3*$^{+/+}$ (open square) or *Smad2*$^{-/-}$*Smad3*$^{+/+}$ (closed square) naive CD4$^+$ T cells were cultured in the iTreg-skewing condition and collected everyday. Cells were fixed, stained for intracellular Foxp3, and assessed by FACS. A bar graph shows the percentage of Foxp3$^+$ cells. Data shown resulted from experiments that were repeated three times with similar results. *C*, FACS-sorted nTregs from control (*Smad2*$^{+/+}$*Smad3*$^{+/+}$), *Smad2*-cKO (*Smad2*$^{-/-}$*Smad3*$^{+/+}$), *Smad3*-KO (*Smad2*$^{+/+}$*Smad3*$^{-/-}$), and 2cKO/3hetero (*Smad2*$^{-/-}$*Smad3*$^{+/-}$) mice were stimulated by anti-CD3e/CD28 with 20 ng/ml of IL-2 in the absence or presence of TGF-β1 for 4 d. Cells were fixed, stained for intracellular Foxp3, and assessed by flow cytometry. Data are representative of two independent experiments with consistent results.

littermate mice (Fig. 7*C*). Reduced Th17 cells in *Smad2*-cKO mice might be due to upregulation of such anti-Th17 inflammatory cytokines (45, 46).

To investigate this possibility, we examined the levels of cytokines in vitro under Th17-skewing conditions. *Smad2*$^{-/-}$*Smad3*$^{+/+}$ CD4$^+$ T cells produced lower levels of IL-17, but produced higher levels of IL-2, IFN-γ and IL-4 than did *Smad2*$^{+/+}$*Smad3*$^{+/+}$ CD4$^+$ T cells (Fig. 7*D*). Intracellular FACS analysis revealed that production of IL-17 was severely reduced in *Smad2*$^{-/-}$*Smad3*$^{+/+}$ and *Smad2*$^{+/+}$*Smad3*$^{-/-}$ CD4$^+$ T cells (Fig. 7*E*, *upper panels*). *Smad2*$^{-/-}$*Smad3*$^{-/-}$ CD4$^+$ T cells were most severely affected (Fig. 7*E*, *upper panels*). Next, we examined the effect of anti–IL-2 Ab on Th17 differentiation. Anti–IL-2 Ab alone efficiently reduced the levels of both IFN-γ and IL-4 production (data not shown). As shown in Fig. 7*E* (*lower panels*), Smad2- or Smad3-deficient CD4$^+$ T cells effectively developed into Th17 cells when anti–IL-2 Ab was included in the culture. We observed significant TH17 development in *Smad2*$^{-/-}$*Smad3*$^{-/-}$ CD4$^+$ T cells. These